

Next-to-next-to-leading order approximation to perturbative QCD at the LHC

Kirill Melnikov

TTP KIT

KITP Santa Barbara, April 7th 2016

Outline

- 1) Some comments on the NNLO QCD approximation
- 2) Example 1: the Higgs width determination at the LHC
- 3) Example 2: Higgs production in association with a jet
- 4) Conclusion

Remarks on NNLO QCD approximation

For the purposes of describing hard processes at colliders, NNLO is better than NLO that is better than LO that is better than a parton shower.

The NNLO QCD approximation is an expansion of the leading twist contribution to proton-proton scattering in the strong coupling constant. The twist expansion itself is quite separate and rarely discussed approximation.

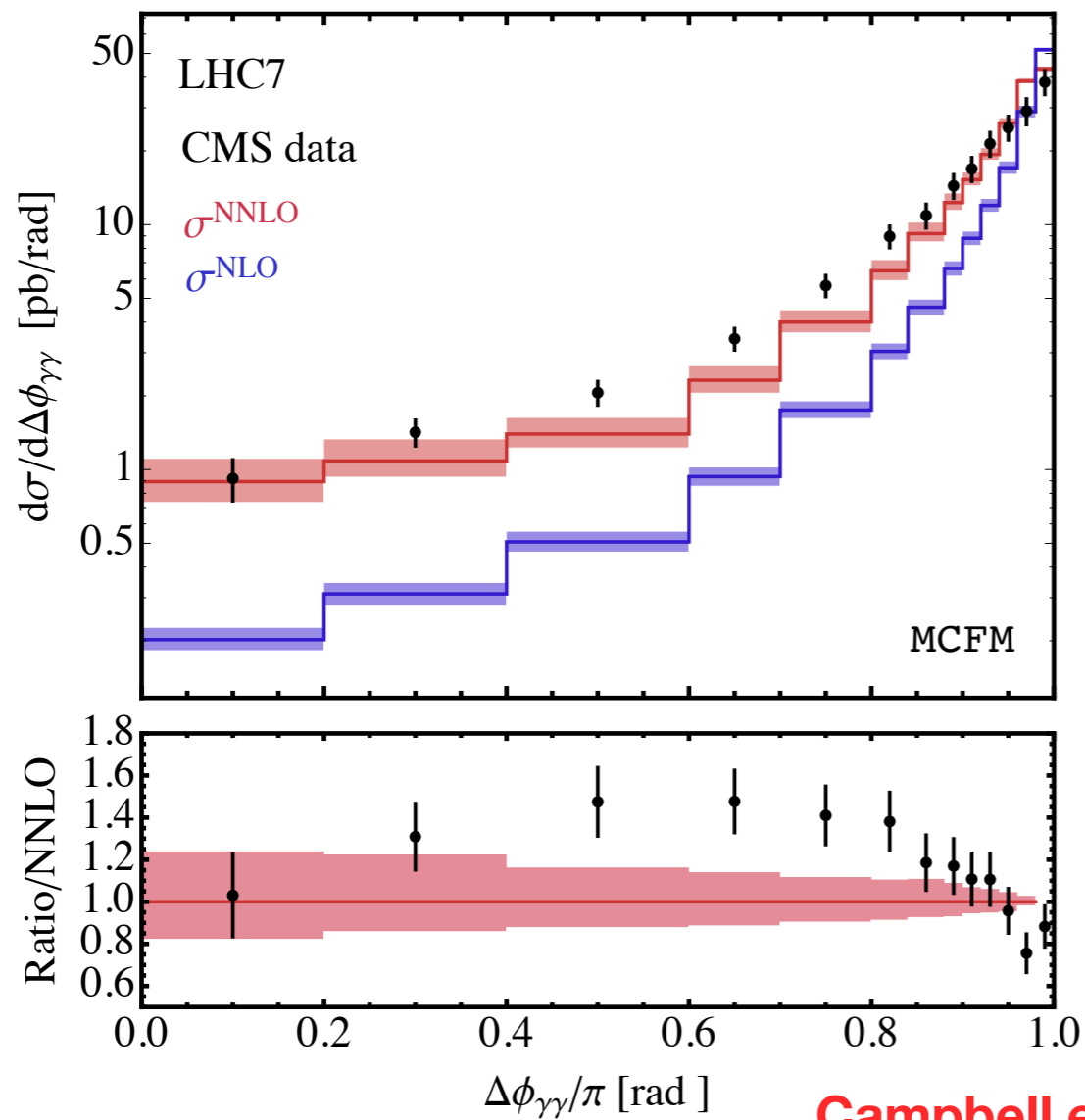
Continuous increase in the “number of N’s” is not possible without hitting a non-perturbative boundary. I do not know where this boundary is and what to do about it, but an idea that one can measure the W mass to 10 MeV (0.01 percent) or the top quark mass to better than 500 MeV (0.3 percent) without addressing non-perturbative effects theoretically from first principles seems disturbing to me.

$$N_c^2 \left(\frac{\alpha_s}{\pi} \right)^2 L_Q^2 \sim \frac{\Lambda_{\text{QCD}}}{Q}$$

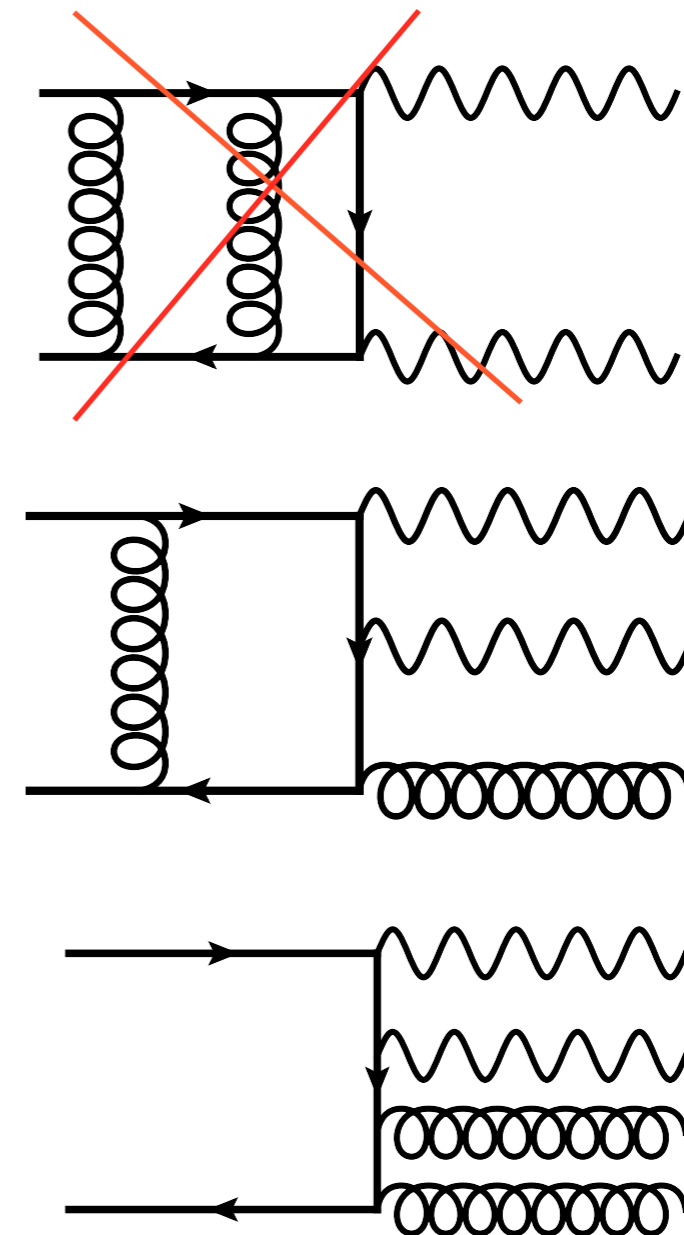
$$d\sigma = \int dx_1 dx_2 f_i(x_1) f_j(x_2) d\sigma_{\text{part}}(x_1 x_2 s_{\text{hadr}})$$

NNLO ≥ 2 loops !

Existence of a NNLO calculation for a process does not imply that any observable computed using a particular "NNLO" code has the NNLO accuracy (pt of the Z in NNLO Drell-Yan, pt of the top pair in NNLO tT production etc.). Sometimes NLO to a higher multiplicity process is more useful than NNLO to a lower multiplicity process.

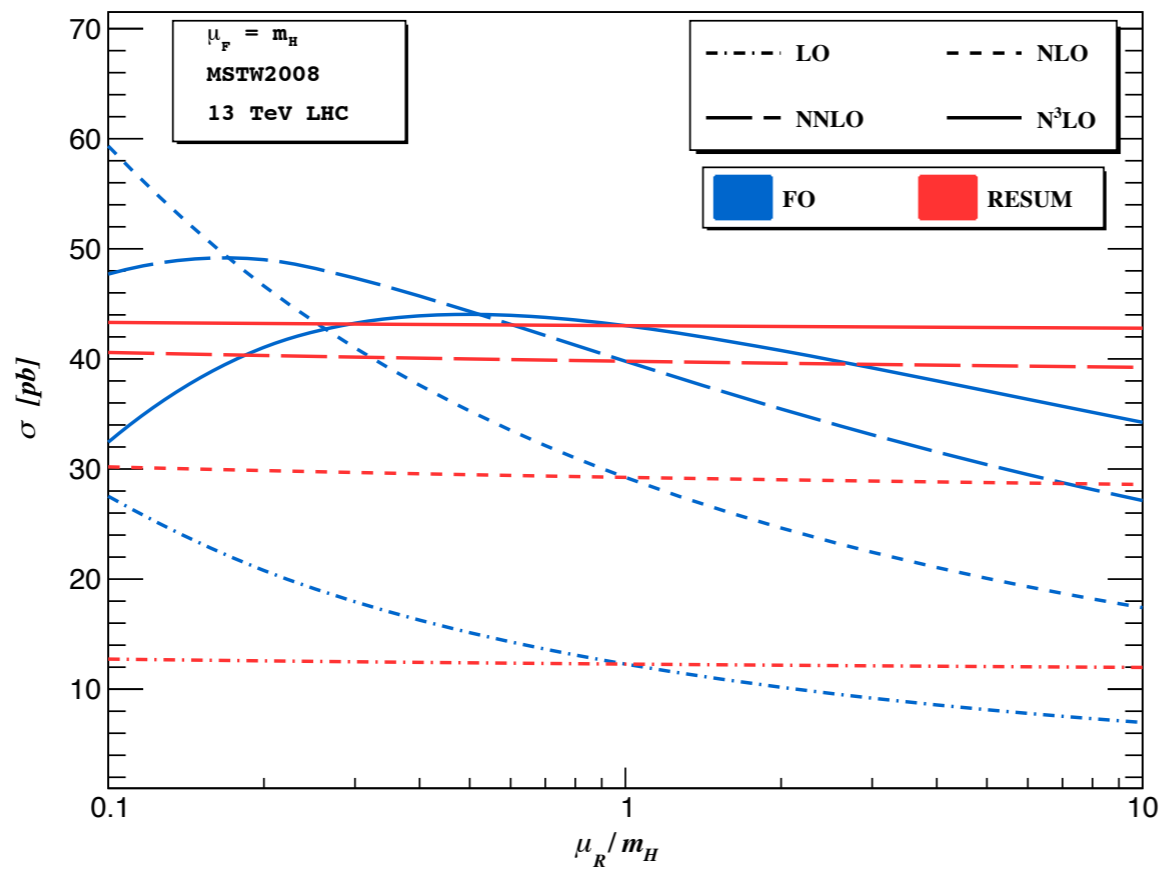


Campbell et al.



Scales

NNLO computations are fairly insensitive to scale choices, at least in the region where NNLO is at work. Too much of a scale choice game can be counter-productive since scale variation uncertainty is one of the few handles we have to understand how relevant of higher order corrections.



	LO	NLO	NNLO	N ³ LO
FO (%)	167.26	143.40	54.99	27.01
RESUM (%)	6.11	5.47	3.39	1.23

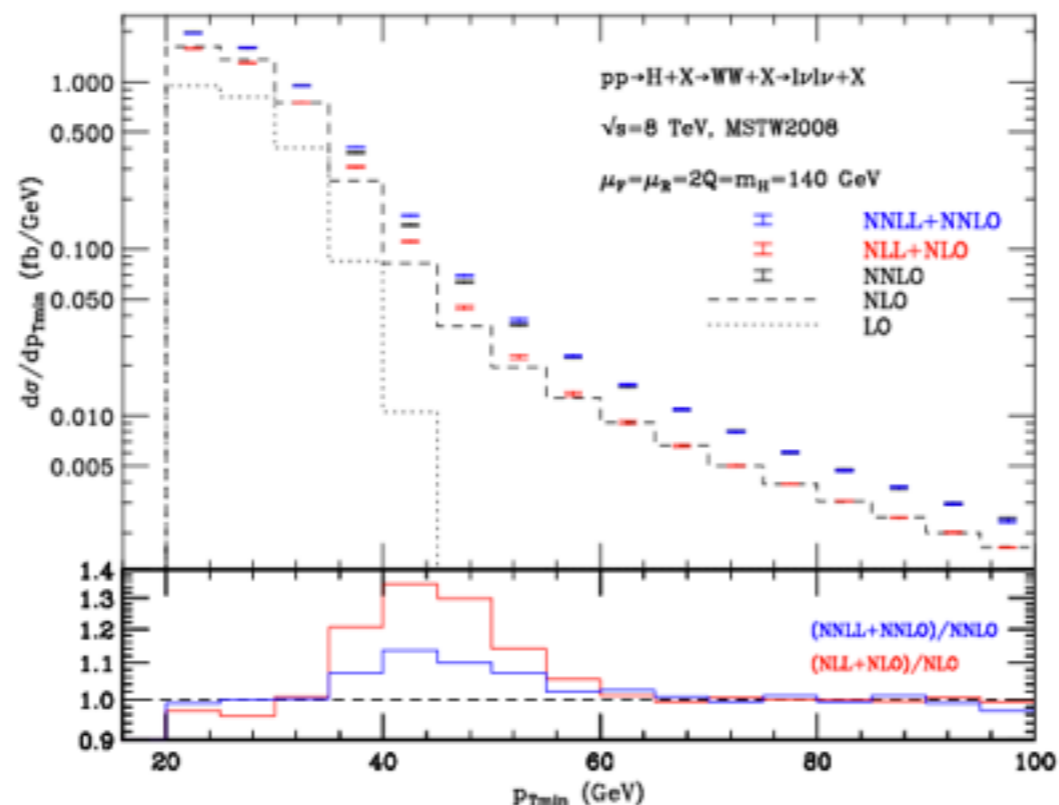
Ahmed et al.

Remarks on NNLO QCD approximation

There seems to be a close proximity of resummed and fixed order computations for realistic selection criteria at the LHC. We are in the “grey” region where both approaches can be used for reasonable estimates of radiative corrections, provided that we can reach sufficiently high orders in the strong coupling expansion.

The main advantage of fixed-order computations is the possibility to compute fiducial cross sections for realistic selection criteria.

The main advantage of resummed computations is that they can be continued to regions where fixed order computations fail. This is good but we rarely need those regions for anything but the consistency checks of the SM.



De Florian et al.

Processes currently known through NNLO

dijets	$O(3\%)$	gluon-gluon, gluon-quark	PDFs, strong couplings, BSM
H+0 jet	$O(3-5 \%)$	fully inclusive (N3LO)	Higgs couplings
H+1 jet	$O(7\%)$	fully exclusive; Higgs decays, infinite mass tops	Higgs couplings, Higgs p_t , structure for the ggH vertex.
tT pair	$O(4\%)$	fully exclusive, stable tops	top cross section, mass, p_t , FB asymmetry, PDFs, BSM
single top	$O(1\%)$	fully exclusive, stable tops, t-channel	V_{tb} , width, PDFs
WBF	$O(1\%)$	exclusive, VBF cuts	Higgs couplings
W+j	$O(1\%)$	fully exclusive, decays	PDFs
Z+j	$O(1-3\%)$	decays, off-shell effects	PDFs
ZH	$O(3-5 \%)$	decays to bb at NLO	Higgs couplings (H-> bb)
ZZ	$O(4\%)$	fully exclusive	Trilinear gauge couplings, BSM
WW	$O(3\%)$	fully inclusive	Trilinear gauge couplings, BSM
top decay	$O(1-2 \%)$	exclusive	Top couplings
H -> bb	$O(1-2 \%)$	exclusive, massless	Higgs couplings, boosted

Ingredients for NNLO computations

A NNLO QCD computation is, essentially, a two-loop computation. However, in theories with massless particles, two-loop computations are insufficient for obtaining a physical answer: two-loop computations need to be combined with contributions of higher-multiplicity processes to physical observables.

Suppose we want to compute the NNLO QCD correction to a process $pp \rightarrow X$. To do this, we need:

- a) two-loop scattering amplitudes for a process X ;
- b) one-loop amplitudes for a process $X+g$;
- d) tree-level amplitudes for a process $X+gg, X+q\bar{q}$ etc.

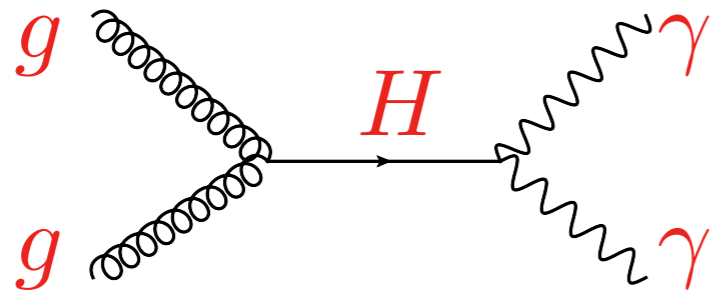
Computation of two-loop scattering amplitudes is a significant challenge;

Integration of tree-level amplitudes over available phase-space requires some procedure that allows an extraction of infra-red divergences (subtraction/slicing techniques).

One-loop amplitudes need to be known in an unresolved region; although one loop computations are "standard" by now, they are not easy especially in unresolved regions.

What is the width of the Higgs boson?

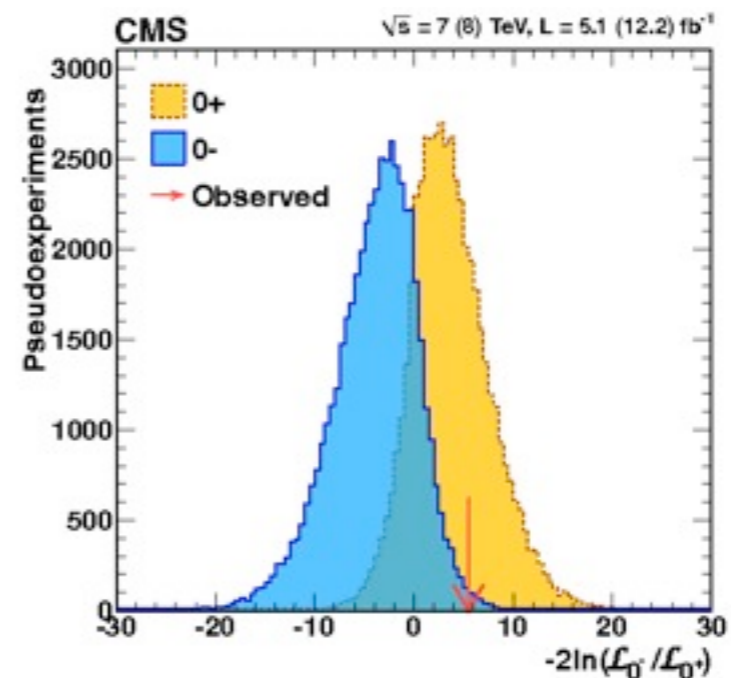
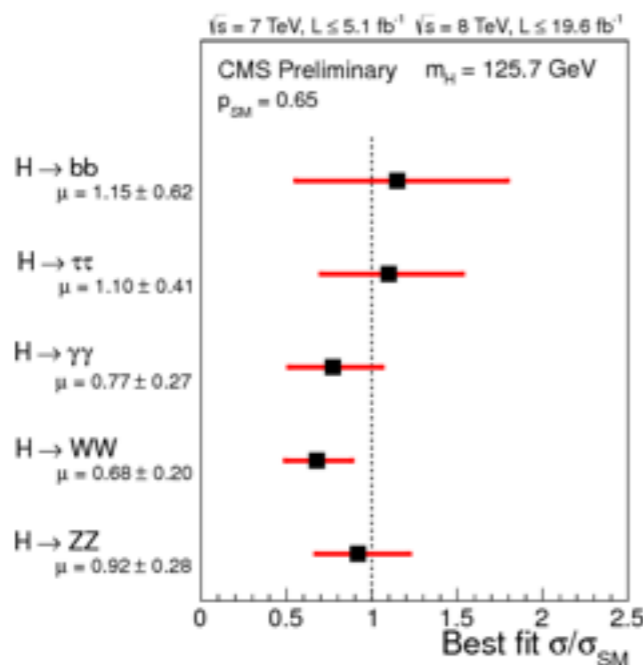
Although many properties of the Higgs bosons appear to be consistent with the Standard Model, reaching this conclusion requires hidden assumptions. One of such assumptions is the Standard Model value of the Higgs boson width.



$$\sigma_{i \rightarrow H \rightarrow f} \sim \frac{g_i^2 g_f^2}{\Gamma_H}$$

The on-shell production cross section is invariant under a simultaneous change of the couplings and the width, resulting in infinitely many solutions. To break the degeneracy, one should find the way to measure the couplings and the width independently of each other.

$$g \rightarrow \xi g, \quad \Gamma_H \rightarrow \xi^4 \Gamma_H \quad \Rightarrow \quad \sigma_H \rightarrow \sigma_H$$



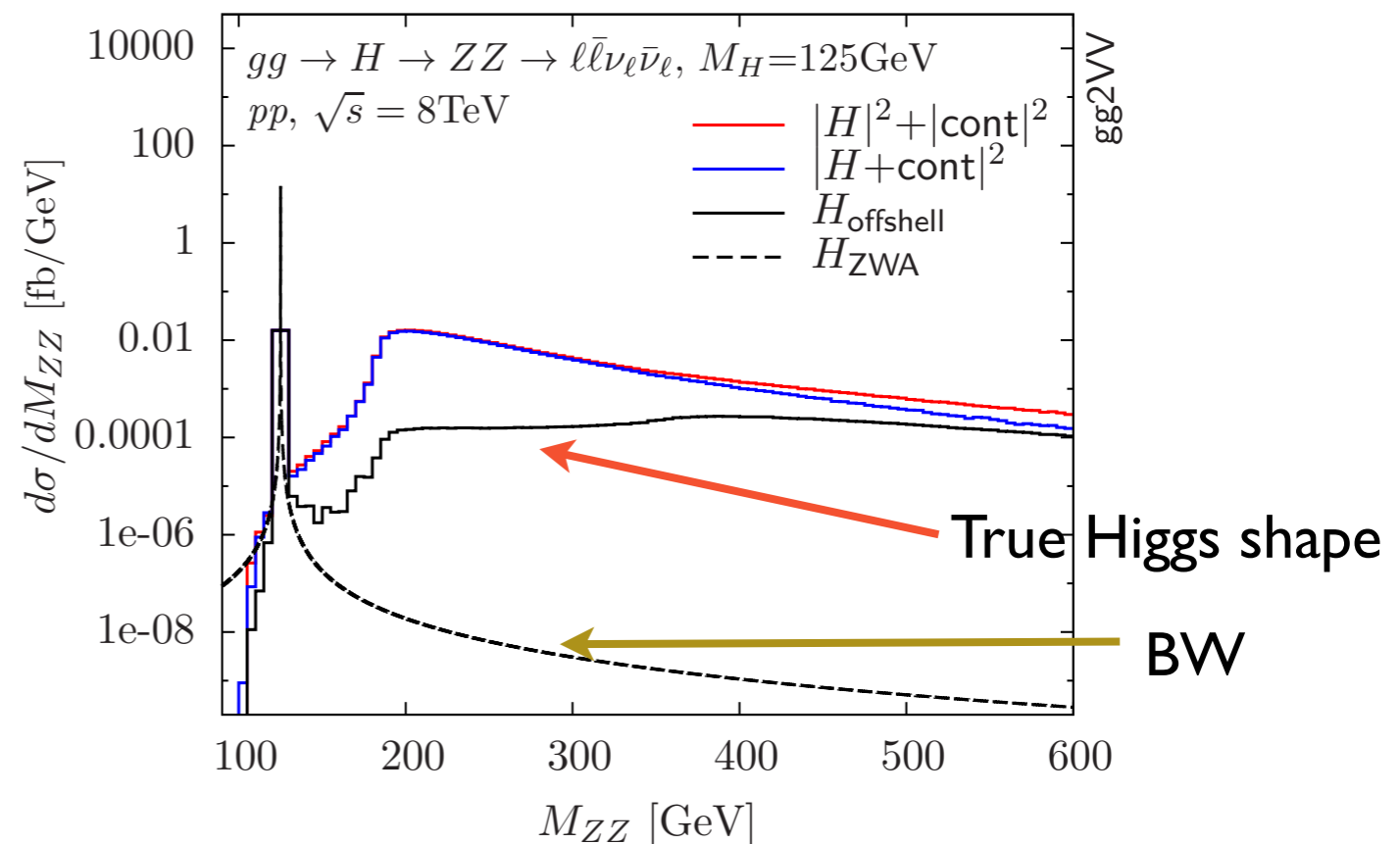
Couplings from off-shell production

One can try to measure the couplings of the Higgs boson when it is produced off-shell. The off-shell cross-section is proportional to Higgs couplings and is independent of the width; this resolves the width/couplings ambiguity.

$$\sigma_{i \rightarrow H \rightarrow f} \sim \int \frac{ds \, g_i^2 g_f^2}{(s - m_h)^2 + m_h^2 \Gamma_h^2} \Big|_{s \gg m_h^2} \rightarrow \frac{g_i^2 g_f^2}{s}$$

The immediate problem with this idea is that off-shell contribution to Higgs boson production is expected to be extremely small.

However, **Kauer and Passarino** pointed out that a significant enhancement in the off-shell Higgs production rate exists, making the invariant mass distribution very different from the expected Breit-Wigner shape.



Kauer, Passarino

Higgs decays to ZZ

One can use this enhancement in the off-shell Higgs production to resolve the couplings/width degeneracy. The cleanest final state is ZZ (four leptons), so it is natural to look there.

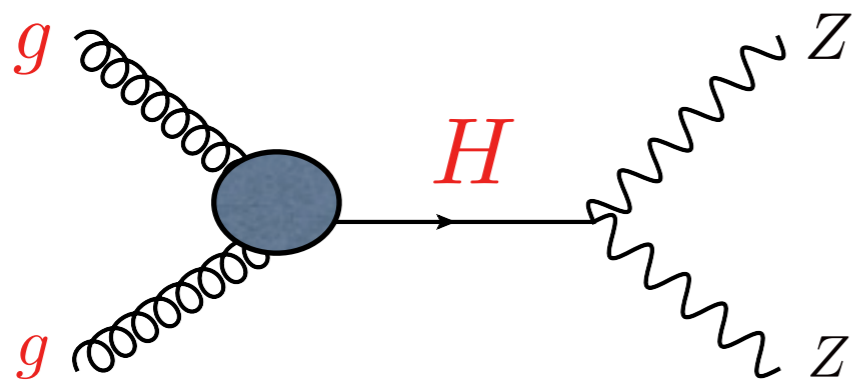
Caola, K.M.

In this case, the off-shell rate appears to be significant because decay to two on-shell Z bosons opens up and because the cross-section for producing two longitudinally polarized Z bosons in decays of (strongly) off-shell Higgs is large.

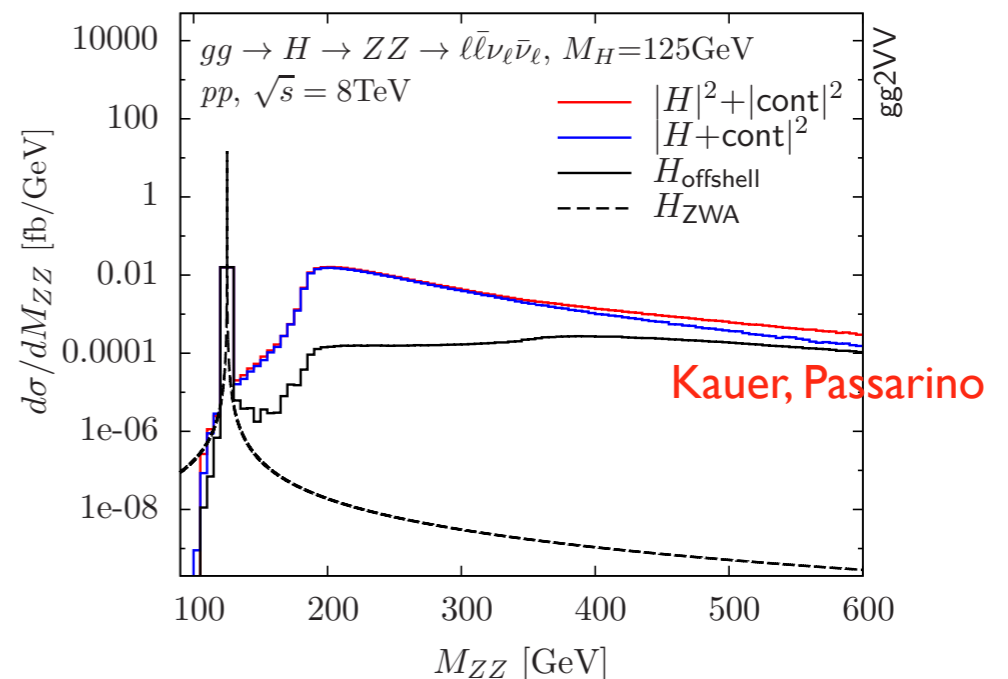
Kauer, Passarino

$$\mathcal{A}_{H^* \rightarrow Z_L Z_L} \sim \frac{s}{v} \quad \frac{|\mathcal{A}_{H^* \rightarrow Z_L Z_L}|^2}{(s - m_h^2)^2 + m_h^2 \Gamma_h^2} \rightarrow \text{const}, \quad s \gg m_h^2$$

For large invariant masses of the Z boson pair, the amplitude divided by the Higgs propagator becomes independent of ZZ invariant mass, enhancing the off-shell production significantly. Numerically, the off-shell production cross section is really significant; it is close to ten percent of the resonance cross-section.

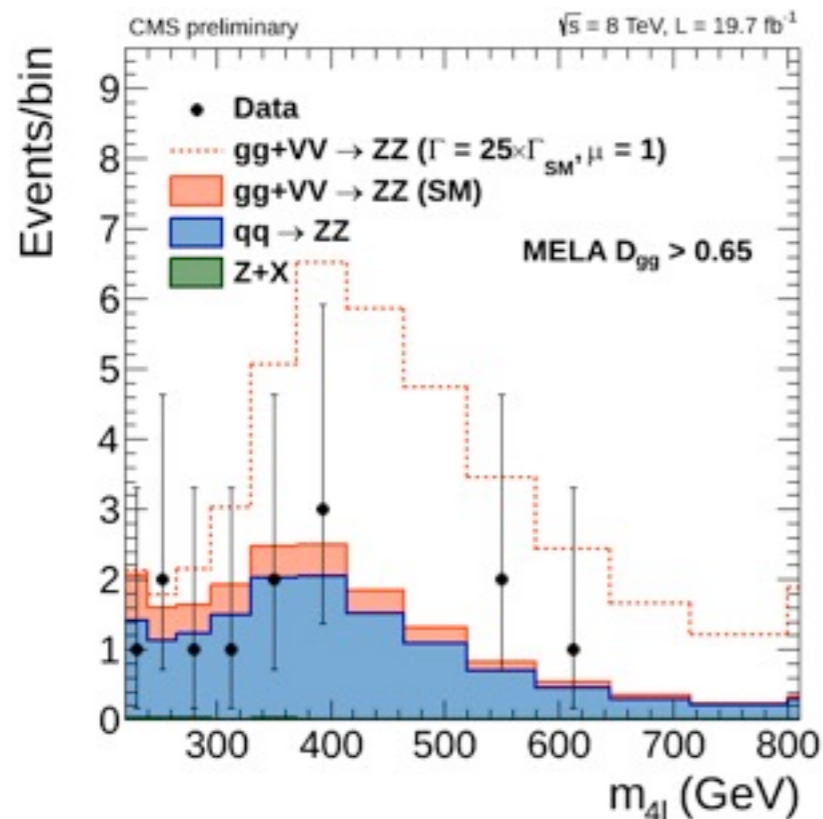


$$\sigma_H(m_{ZZ} > 160 \text{ GeV}) \approx 0.1 \sigma_H$$



The Higgs width constraint: CMS

CMS collaboration measured the number of 4-lepton events in the off-shell region and used it to constrain the Higgs width. The measurement includes both ZZ and WW channels.



		4ℓ	$2\ell 2\nu$
(a)	total gg ($\Gamma_H = \Gamma_H^{\text{SM}}$)	1.8 ± 0.3	9.6 ± 1.5
	gg signal component ($\Gamma_H = \Gamma_H^{\text{SM}}$)	1.3 ± 0.2	4.7 ± 0.6
	gg background component	2.3 ± 0.4	10.8 ± 1.7
(b)	total gg ($\Gamma_H = 10 \times \Gamma_H^{\text{SM}}$)	9.9 ± 1.2	39.8 ± 5.2
(c)	total VBF ($\Gamma_H = \Gamma_H^{\text{SM}}$)	0.23 ± 0.01	0.90 ± 0.05
	VBF signal component ($\Gamma_H = \Gamma_H^{\text{SM}}$)	0.11 ± 0.01	0.32 ± 0.02
	VBF background component	0.35 ± 0.02	1.22 ± 0.07
(d)	total VBF ($\Gamma_H = 10 \times \Gamma_H^{\text{SM}}$)	0.77 ± 0.04	2.40 ± 0.14
(e)	$q\bar{q}$ background	9.3 ± 0.7	47.6 ± 4.0
(f)	other backgrounds	0.05 ± 0.02	35.1 ± 4.2
(a+c+e+f)	total expected ($\Gamma_H = \Gamma_H^{\text{SM}}$)	11.4 ± 0.8	93.2 ± 6.0
(b+d+e+f)	total expected ($\Gamma_H = 10 \times \Gamma_H^{\text{SM}}$)	20.1 ± 1.4	124.9 ± 7.8
	observed	11	91

$$\Gamma_H < 5.4 \Gamma_{H,\text{SM}} = 22 \text{ MeV @ 95CL}$$

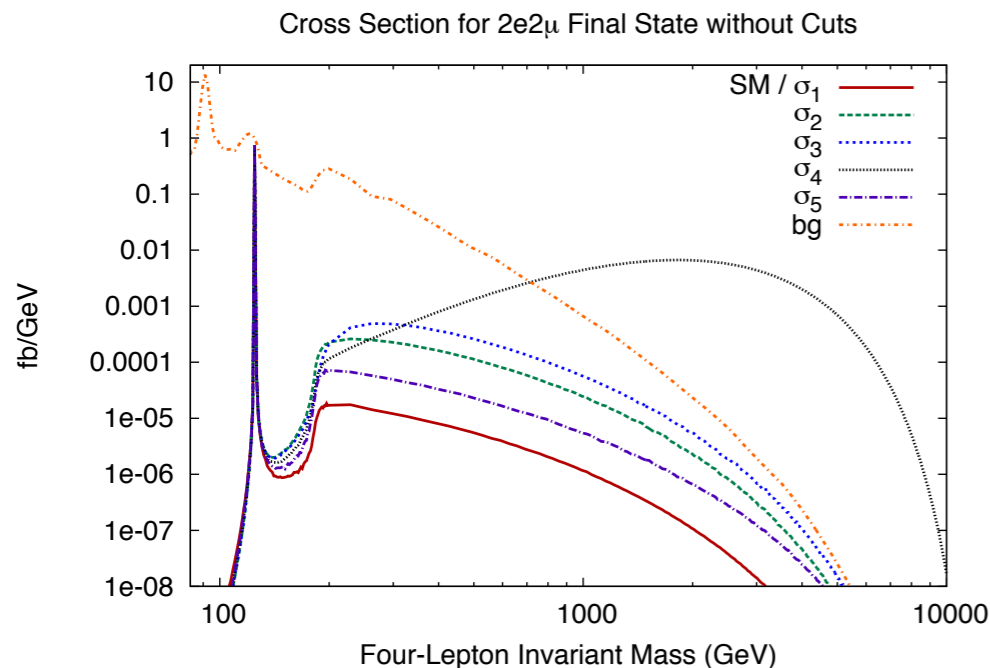
A very impressive result -- almost two orders of magnitude improvement compared to the direct (on peak) bound of the width.

New predictions for background processes

To verify the consistency of the off-shell production regime with the Standard Model nature of the Higgs boson as precisely as possible, we need to predict the number of four-lepton events at high ZZ -invariant mass accurately.

To understand what precision is needed, it is instructive to keep in mind that in the current (8 TeV) 4-lepton analysis, CMS expects 11 off-shell events in the SM and that 1 event, out of these 11, is caused by the off-shell Higgs boson, 2 event are caused by $gg \rightarrow ZZ$ and -1 event by the interference. The rest is $qqb \rightarrow ZZ$.

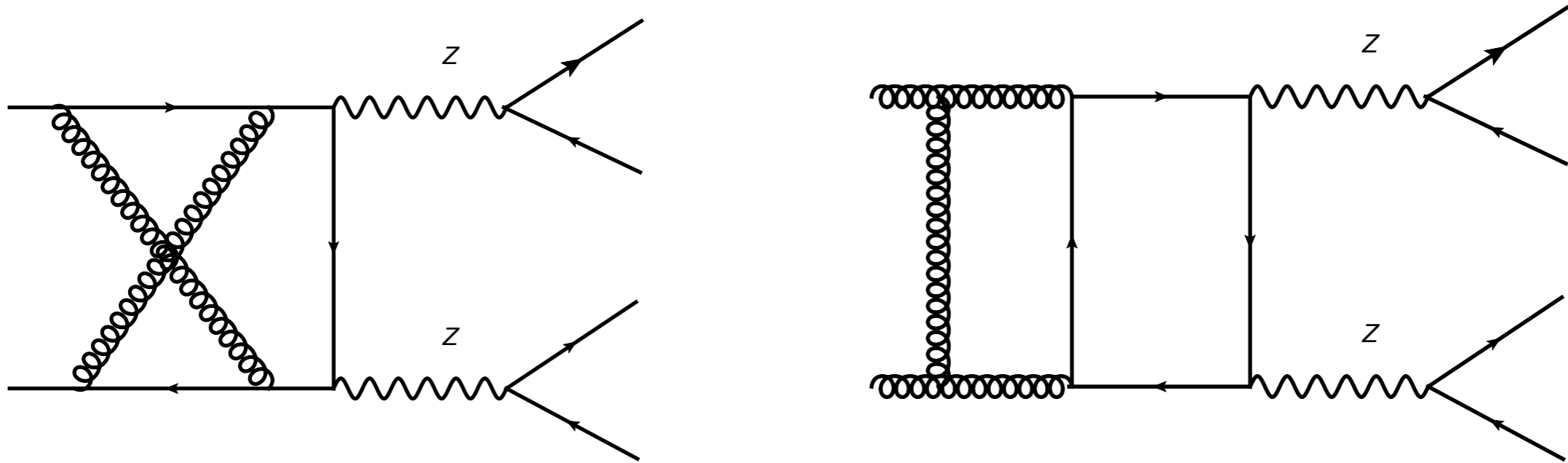
This implies that if we want to constrain the couplings to $O(20\%)$ (and the width within a factor of two), $O(10\%)$ prediction for $qq \rightarrow ZZ$ and $O(50\%)$ prediction for $gg \rightarrow ZZ$ is required. **This was an important challenge but we have almost reached it !**



		4ℓ	$2\ell 2\nu$
(a)	total gg ($\Gamma_H = \Gamma_H^{\text{SM}}$)	1.8 ± 0.3	9.6 ± 1.5
	gg signal component ($\Gamma_H = \Gamma_H^{\text{SM}}$)	1.3 ± 0.2	4.7 ± 0.6
	gg background component	2.3 ± 0.4	10.8 ± 1.7
(b)	total gg ($\Gamma_H = 10 \times \Gamma_H^{\text{SM}}$)	9.9 ± 1.2	39.8 ± 5.2
(c)	total VBF ($\Gamma_H = \Gamma_H^{\text{SM}}$)	0.23 ± 0.01	0.90 ± 0.05
	VBF signal component ($\Gamma_H = \Gamma_H^{\text{SM}}$)	0.11 ± 0.01	0.32 ± 0.02
	VBF background component	0.35 ± 0.02	1.22 ± 0.07
(d)	total VBF ($\Gamma_H = 10 \times \Gamma_H^{\text{SM}}$)	0.77 ± 0.04	2.40 ± 0.14
(e)	$q\bar{q}$ background	9.3 ± 0.7	47.6 ± 4.0
(f)	other backgrounds	0.05 ± 0.02	35.1 ± 4.2
(a+c+e+f)	total expected ($\Gamma_H = \Gamma_H^{\text{SM}}$)	11.4 ± 0.8	93.2 ± 6.0
(b+d+e+f)	total expected ($\Gamma_H = 10 \times \Gamma_H^{\text{SM}}$)	20.1 ± 1.4	124.9 ± 7.8
	observed	11	91

NNLO QCD predictions for the background

NNLO QCD predictions for ZZ production require computation of complicated two-loop scattering amplitudes.



These are computed using the standard steps that include: parametrization of amplitudes in terms of Lorentz-invariant form factors; reduction to master integrals followed by the calculation of master integrals.

Interestingly, with these standard procedures, we are getting to the point where these computations become hardly manageable (the amplitude depends on four kinematic invariants).

gg -> VV scattering amplitude

As an illustration, consider computation of a two-loop gg -> VV amplitude. For generic vector bosons, the amplitude can be written in a form with all electroweak couplings factored out (**massless quarks only**)

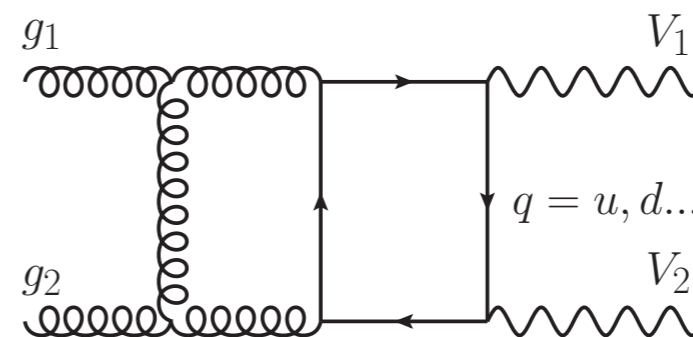
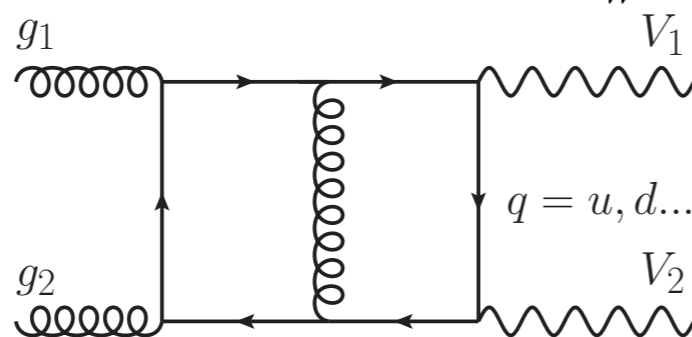
$$\mathcal{M}(\lambda_{g_1}, \lambda_{g_2}, \lambda_5, \lambda_7) = i \left(\frac{g_W}{\sqrt{2}} \right)^4 \delta^{a_1 a_2} \mathcal{D}_3 \mathcal{D}_4 C_{l, V_2}^{\lambda_7} C_{l, V_1}^{\lambda_5} \epsilon_3^\mu(\lambda_5) \epsilon_4^\nu(\lambda_7) C_{V_1 V_2} \mathcal{A}_{\mu\nu}(p_1^{\lambda_{g_1}}, p_2^{\lambda_{g_2}}; p_3, p_4),$$

Couplings to leptons and quarks are shown below; **note the absence of vector-axial current correlators (C-parity) and the equality of the vector-vector and axial-axial current correlators.**

$$C_\gamma^{L,R} = -\sqrt{2} Q_l \sin \theta_W, \quad C_{l,Z}^{L,R} = \frac{1}{\sqrt{2} \cos \theta_W} (V_l \pm A_l), \quad C_{lW^+}^\lambda = C_{lW^-}^\lambda = \delta_{\lambda L}.$$

$$V_e = -1/2 + 2 \sin^2 \theta_W, \quad V_\nu = 1/2, \quad A_e = -1/2, \quad A_\nu = 1/2$$

$$C_{\gamma\gamma} = \frac{20 \sin^2 \theta_W}{9}, \quad C_{ZZ} = \frac{(V_u^2 + V_d^2 + A_u^2 + A_d^2)}{\cos^2 \theta_W}, \quad C_{Z\gamma} = -\frac{2 \sin \theta_W}{\cos \theta_W} (V_u Q_u + V_d Q_d), \quad C_{W^+W^-} = 1,$$



The primary object to compute is the amplitude $A(p_1, p_2, p_3, p_4)$ contracted with the polarization vectors of vector bosons. Only vector couplings of electroweak bosons are needed.

gg -> VV scattering amplitude

The problem with computing the amplitude $A(p_1, p_2, p_3, p_4)$ "as is" is that it is too complicated at two-loops. Indeed, integration-by-parts technology can not be used efficiently if there are many external vectors ([vector boson polarizations and/or lepton momenta](#)) in the calculation.

To remove all external vectors, we need to express the amplitude through invariant form factors. If this is done without imposing reasonable physics conditions, the number of form factors becomes very large, $O(150)$!

Using transversality and gauge-fixing conditions $\epsilon_1 \cdot p_{1,2} = 0$, $\epsilon_2 \cdot p_{1,2} = 0$, $\epsilon_3 \cdot p_3 = 0$, $\epsilon_4 \cdot p_4 = 0$. we express the amplitude through just 20 form factors.

$$\begin{aligned} \mathcal{A} = & T_1 (\epsilon_1 \cdot \epsilon_2) (\epsilon_3 \cdot \epsilon_4) + T_2 (\epsilon_1 \cdot \epsilon_3) (\epsilon_2 \cdot \epsilon_4) + T_3 (\epsilon_1 \cdot \epsilon_4) (\epsilon_2 \cdot \epsilon_3) \\ & + (\epsilon_1 \cdot \epsilon_2) (T_4(p_1 \cdot \epsilon_3) (p_1 \cdot \epsilon_4) + T_5(p_1 \cdot \epsilon_3) (p_2 \cdot \epsilon_4) + T_6(p_2 \cdot \epsilon_3) (p_1 \cdot \epsilon_4) + T_7(p_2 \cdot \epsilon_3) (p_2 \cdot \epsilon_4)) \\ & + (\epsilon_1 \cdot \epsilon_3) (p_\perp \cdot \epsilon_2) (T_8(p_1 \cdot \epsilon_4) + T_9(p_2 \cdot \epsilon_4)) + (\epsilon_1 \cdot \epsilon_4) (p_\perp \cdot \epsilon_2) (T_{10}(p_1 \cdot \epsilon_3) + T_{11}(p_2 \cdot \epsilon_3)) \\ & + (\epsilon_2 \cdot \epsilon_3) (p_\perp \cdot \epsilon_1) (T_{12}(p_1 \cdot \epsilon_4) + T_{13}(p_2 \cdot \epsilon_4)) + (\epsilon_2 \cdot \epsilon_4) (p_\perp \cdot \epsilon_1) (T_{14}(p_1 \cdot \epsilon_3) + T_{15}(p_2 \cdot \epsilon_3)) \\ & + (\epsilon_1 \cdot p_\perp) (\epsilon_2 \cdot p_\perp) (T_{17}(p_1 \cdot \epsilon_3) (p_1 \cdot \epsilon_4) + T_{18}(p_1 \cdot \epsilon_3) (p_2 \cdot \epsilon_4) + T_{19}(p_2 \cdot \epsilon_3) (p_1 \cdot \epsilon_4) \\ & + T_{20}(p_2 \cdot \epsilon_3) (p_2 \cdot \epsilon_4)) + (\epsilon_3 \cdot \epsilon_4) (p_\perp \cdot \epsilon_1) (p_\perp \cdot \epsilon_2) T_{16} \end{aligned}$$

The transverse momentum is defined through the Sudakov decomposition w.r.t p_1 and p_2 .

The invariant form-factors T_1 - T_{20} are functions of Mandelstam variables only; if we construct operators that project $A \rightarrow T_{i=1..16}$, we are able to apply integration-by-parts technology without much problem.

gg -> WW scattering amplitude

It is relatively straightforward to construct such projection operators ([their choices are by far not unique](#)). We start by defining an auxiliary object (note projections on physical polarizations)

$$\mathcal{O}^{\mu_1\mu_2\mu_3\mu_4} = \bar{A}_{\nu_1\nu_2\nu_3\nu_4} \mathcal{P}_{12}^{\nu_1\mu_1} \mathcal{P}_{12}^{\nu_2\mu_2} \mathcal{P}_3^{\nu_3\mu_3} \mathcal{P}_4^{\nu_4\mu_4}.$$

$$\mathcal{P}_{12}^{\mu\nu} = -g^{\mu\nu} + \frac{p_1^\mu p_2^\nu + p_1^\nu p_2^\mu}{p_1 \cdot p_2}, \quad \mathcal{P}_3^{\mu\nu} = -g^{\mu\nu} + \frac{p_3^\mu p_3^\nu}{p_3^2}, \quad \mathcal{P}_4^{\mu\nu} = -g^{\mu\nu} + \frac{p_4^\mu p_4^\nu}{p_4^2}.$$

We then contract it with various vectors and tensors and find a mapping $G_{1..20} \rightarrow T_{1..20}$

$$G_1 = \mathcal{O}^{\mu_1\mu_2\mu_3\mu_4} g_{\mu_1\mu_2} g_{\mu_3\mu_4},$$

$$G_2 = \mathcal{O}^{\mu_1\mu_2\mu_3\mu_4} g_{\mu_1\mu_3} g_{\mu_2\mu_4},$$

$$G_3 = \mathcal{O}^{\mu_1\mu_2\mu_3\mu_4} g_{\mu_1\mu_4} g_{\mu_2\mu_3},$$

$$G_4 = p_\perp^{-4} s^{-2} \mathcal{O}^{p_\perp p_\perp p_1 p_1},$$

$$G_5 = p_\perp^{-4} s^{-2} \mathcal{O}^{p_\perp p_\perp p_1 p_2},$$

$$G_6 = p_\perp^{-4} s^{-2} \mathcal{O}^{p_\perp p_\perp p_2 p_1},$$

$$G_7 = p_\perp^{-4} s^{-2} \mathcal{O}^{p_\perp p_\perp p_2 p_2},$$

$$G_8 = 4p_\perp^{-6} s^{-2} \mathcal{O}^{p_\perp p_\perp \mu_3 \mu_4} t_{\mu_3 \mu_4},$$

$$G_9 = 4p_\perp^{-6} s^{-6} \mathcal{O}^{\mu_1 \mu_2 p_1 p_1} t_{\mu_1 \mu_2},$$

$$G_{10} = 8p_\perp^{-4} s^{-3} \mathcal{O}^{p_\perp \mu_2 \mu_3 p_1} t_{\mu_2 \mu_3},$$

$$G_{11} = 4p_\perp^{-6} s^{-3} \mathcal{O}^{p_\perp \mu_2 \mu_3 p_\perp} t_{\mu_2 \mu_3},$$

$$G_{12} = 8p_\perp^{-4} s^{-3} \mathcal{O}^{\mu_1 p_\perp p_1 \mu_4} t_{\mu_1, \mu_4},$$

$$G_{13} = 4p_\perp^{-6} s^{-3} \mathcal{O}^{\mu_1 p_\perp p_\perp \mu_4} t_{\mu_1, \mu_4},$$

$$G_{14} = 8p_\perp^{-4} s^{-3} \mathcal{O}^{\mu_1 p_\perp \mu_3 p_2} t_{\mu_1, \mu_3},$$

$$G_{15} = 4p_\perp^{-6} s^{-3} \mathcal{O}^{\mu_1 p_\perp \mu_3 p_\perp} t_{\mu_1, \mu_3},$$

$$G_{16} = 8p_\perp^{-4} s^{-3} \mathcal{O}^{p_\perp \mu_2 p_1 \mu_4} t_{\mu_2, \mu_4},$$

$$G_{17} = 4p_\perp^{-6} s^{-3} \mathcal{O}^{p_\perp \mu_2 p_\perp \mu_4} t_{\mu_2, \mu_4},$$

$$G_{18} = 4p_\perp^{-6} s^{-6} \mathcal{O}^{\mu_1 \mu_2 p_1 p_2} t_{\mu_1 \mu_2},$$

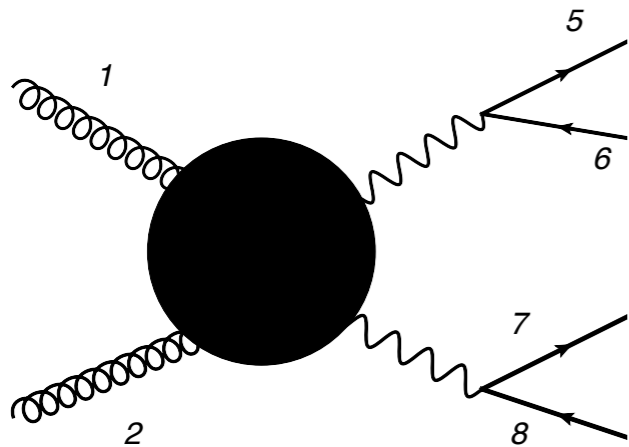
$$G_{19} = 4p_\perp^{-6} s^{-6} \mathcal{O}^{\mu_1 \mu_2 p_2 p_1} t_{\mu_1 \mu_2},$$

$$G_{20} = 4p_\perp^{-6} s^{-6} \mathcal{O}^{\mu_1 \mu_2 p_2 p_2} t_{\mu_1 \mu_2}.$$

$$t_{\nu_1}^{\mu_1} = \delta_{\nu_1 p_1 p_2 p_\perp}^{\mu_1 p_1 p_2 p_\perp} = \delta_{\nu_1 \nu_2 \nu_3 \nu_4}^{\mu_1 \mu_2 \mu_3 \mu_4} p_1^{\nu_2} p_2^{\nu_3} p_\perp^{\nu_4} p_{1, \mu_2} p_{2, \mu_3} p_{\perp, \mu_4} \quad \delta_{\nu_1 \nu_2 \nu_3 \nu_4}^{\mu_1 \mu_2 \mu_3 \mu_4} = \det |g_{\nu_j}^{\mu_i}|.$$

gg -> VV scattering amplitude

It turns out that it is easier to construct **helicity amplitudes** from projections that we just described; one requires **just two independent helicity amplitudes** (polarizations of gluons are either the same or different); each amplitude is expressed in terms of nine form factors. Vector boson polarization vectors are $\epsilon_3^\mu = \langle 5 | \gamma^\mu | 6 \rangle$, $\epsilon_4^\mu = \langle 7 | \gamma^\mu | 8 \rangle$.



$$\begin{aligned} \mathcal{A}_{3L4L}^{\lambda_1 \lambda_2} = & \mathcal{N}_{\lambda_1 \lambda_2} \left\{ \left(F_1^{\lambda_1 \lambda_2} \langle 15 \rangle [61] + F_2^{\lambda_1 \lambda_2} \langle 25 \rangle [62] \right) \langle 17 \rangle [81] \right. \\ & + \left(F_3^{\lambda_1 \lambda_2} \langle 15 \rangle [61] + F_4^{\lambda_1 \lambda_2} \langle 25 \rangle [62] \right) \langle 27 \rangle [82] + 2F_5^{\lambda_1 \lambda_2} \langle 57 \rangle [86] \\ & + \frac{1}{2} \left(F_6^{\lambda_1 \lambda_2} \langle 15 \rangle [61] + F_7^{\lambda_1 \lambda_2} \langle 25 \rangle [62] \right) \left(\langle 12 \rangle \langle 78 \rangle [81] [82] + \langle 17 \rangle \langle 27 \rangle [21] [87] \right) \\ & \left. - \frac{1}{2} \left(F_8^{\lambda_1 \lambda_2} \langle 17 \rangle [81] + F_9^{\lambda_1 \lambda_2} \langle 27 \rangle [82] \right) \left(\langle 12 \rangle \langle 56 \rangle [61] [62] + \langle 15 \rangle \langle 25 \rangle [21] [65] \right) \right\}. \end{aligned}$$

Examples of relations between F and G form factors are shown below. Note that no spurious d-4 singularities are present in these relations !

$$\begin{aligned} F_6^{LL} &= \frac{(m_3^2 - u)(G_{12} + G_{16})}{(d-3)(m_3^2 - t)} + \frac{s(m_3^2 + p_\perp^2)(G_{13} + G_{17})}{(d-3)(m_3^2 - t)}, \\ F_7^{LL} &= \frac{G_{12} + G_{16} + (t - m_3^2)(G_{13} + G_{17})}{d-3}, \\ F_8^{LL} &= \frac{(m_4^2 - t)G_{10} - s(m_4^2 + p_\perp^2)G_{11}}{(d-3)(m_4^2 - u)} + \frac{G_{14} + (m_4^2 - t)G_{15}}{d-3}, \\ F_9^{LL} &= \frac{(u - m_4^2)G_{11} - G_{10}}{d-3} + \frac{(u - m_4^2)G_{14} + s(m_4^2 + p_\perp^2)G_{15}}{(d-3)(m_4^2 - t)}. \end{aligned}$$

gg \rightarrow VV scattering amplitude

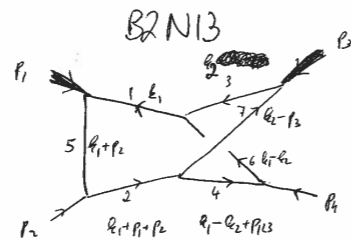
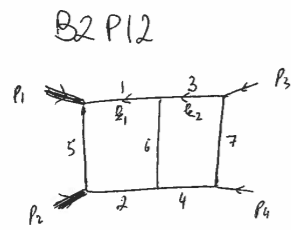
As the result, it appears that form factors can be computed in a straightforward way. We need to:

- 1) generate diagrams (QGRAPH);
- 2) project on relevant operators (Form);
- 3) express the result in terms of various two-loop four-point integrals (Form) ;
- 4) apply integration-by-parts identities to reduce these integrals to master integrals (FIRE);
- 5) combine the results into physical form factors;
- 6) write a numerical program (Fortran,C++) that can turn the analytic formulas into numbers;

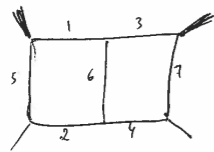
Even if every step sounds straightforward, most of them are non-trivial and demanding. A particular problem is the size of expressions that affects both reduction to master integrals and procession of the final expressions. [For example, the size of Fortran files \(not executables\) for the final two-loop amplitude gg \$\rightarrow\$ \$VV\$ is O\(100 MB\) !\)](#)

The remaining problem to address is the computation of master integrals and this is what we will discuss now.

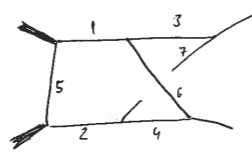
Two-loop virtual corrections: example of $qq \rightarrow V_1 V_2$



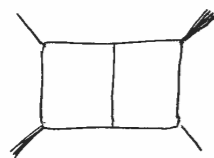
B2P13



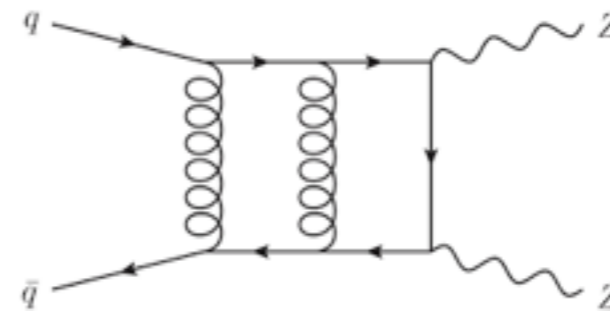
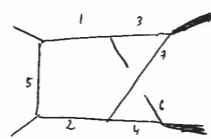
B2N12



B2P23



B2N34



For the case of double vector boson production, we can identify six different two-loop topologies; the differential equations can be “rationalized” with the appropriate change of variables and then solved in terms of the so-called Goncharov polylogarithms.

$$G(a_n, a_{n-1}, \dots, a_1, t) = \int_0^t \frac{dt_n}{t_n - a_n} G(a_{n-1}, \dots, a_1, t_n)$$

$$\frac{s}{m_3^2} = (1+x)(1+xy),$$

$$\sqrt{(s - m_3^2 - m_4^2)^2 - 4m_3^2 m_4^2} = m_3^2 x(1-y)$$

$$\frac{t}{m_3^2} = -xz, \quad \frac{m_4^2}{m_3^2} = x^2 y$$

$$d\vec{f} = \epsilon(dA) \times f, \quad A = \sum A_i \log \alpha_i$$

$$\alpha = \{x, y, z, 1+x, 1-y, 1+xy, z-y, 1+y(1+x)-z, xy+z, 1+x(1+y-z), 1+xz, 1+y-z, z+x(z-y)+xyz, z-y+yz+xyz\}$$

Important and difficult issues:

- 1) finding a suitable basis;
- 2) choice of “rational variables”;
- 3) boundary conditions for differential equations;
- 4) analytic continuation from Euclidean to Minkowski;
- 5) numerical evaluation of Goncharov’s polylogarithms;
- 6) mapping G’s on conventional polylogarithms.

Caola, Henn, Melnikov, Smirnov, Smirnov

Two-loop calculations: amplitudes and integrals

Here are a few things that we learned recently about two-loop computations:

1) Calculation of master integrals using differential equations in kinematic variables is now a method of choice. It has benefited from an understanding of how the bookkeeping in such calculations can be streamlined by choosing appropriate master integrals and working with particular special functions.

Remiddi, Kotikov, Henn, Papadopoulos

2) We are able to successfully study master integrals with up to 4 kinematic invariants and there are indications that even larger number of kinematic invariants can be dealt with.

Gehrmann, Henn, Tancredi, Caola, Smirnov(s), Papadopoulos, Tommasini, Wever

3) Internal masses is a big challenge since they introduce new special functions whose properties are currently being explored.

Weinzierl, Tancredi, Remiddi

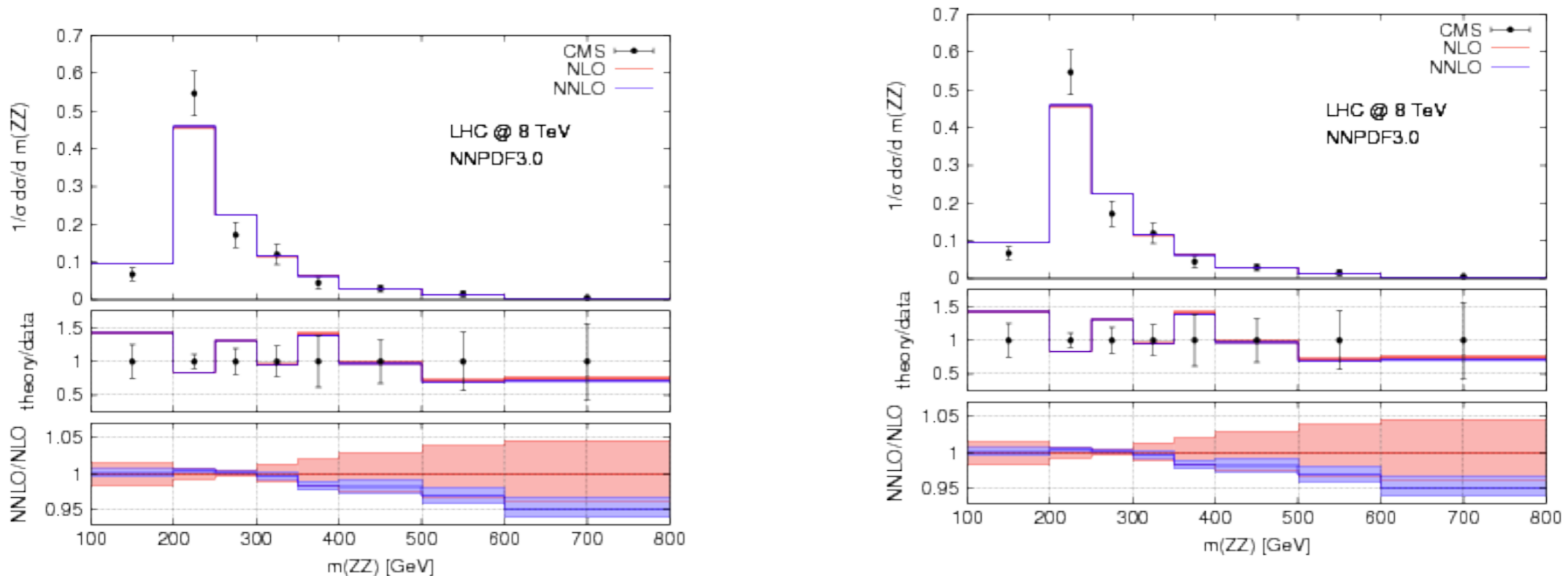
4) There are interesting attempts to understand if two-loop computations can be done using [unitarity techniques](#), that turned out to be so powerful at one-loop. While there was an impressive progress in this field related to classification of integrand residuals based on techniques from algebraic geometry, there are still many outstanding issues.

Badger, Frellesvig, Zhang, Mastrolia, Ita

Z-boson pair production: quark annihilation

The fully-differential production of two Z-bosons in quark-anti-quark annihilation was computed through NNLO QCD, including off-shell effects and decays of the Z-bosons.

The residual uncertainty on the cross section is estimated to be of the order of 3%; this should enable precise predictions for the “background” for the determination of the Higgs boson width. Note that this calculation relies on the two-loop amplitudes for $qq \rightarrow V_1 V_2$ and uses the q_t -subtraction scheme, to combine real and virtual corrections.



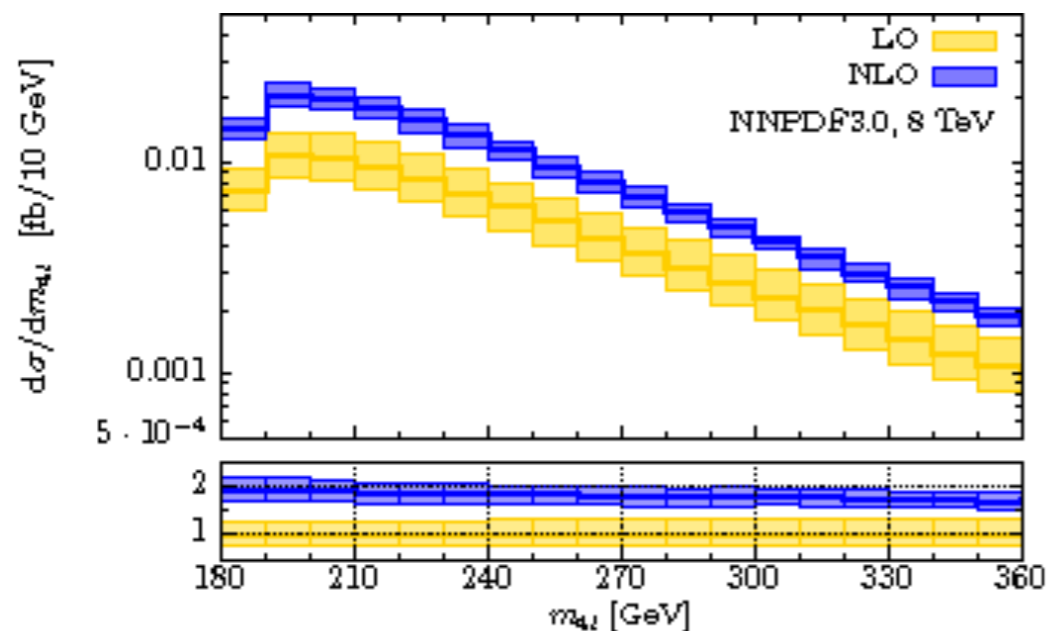
M. Grazzini, S. Kallweit, D. Rathlev

Z-boson pair production: gluon annihilation

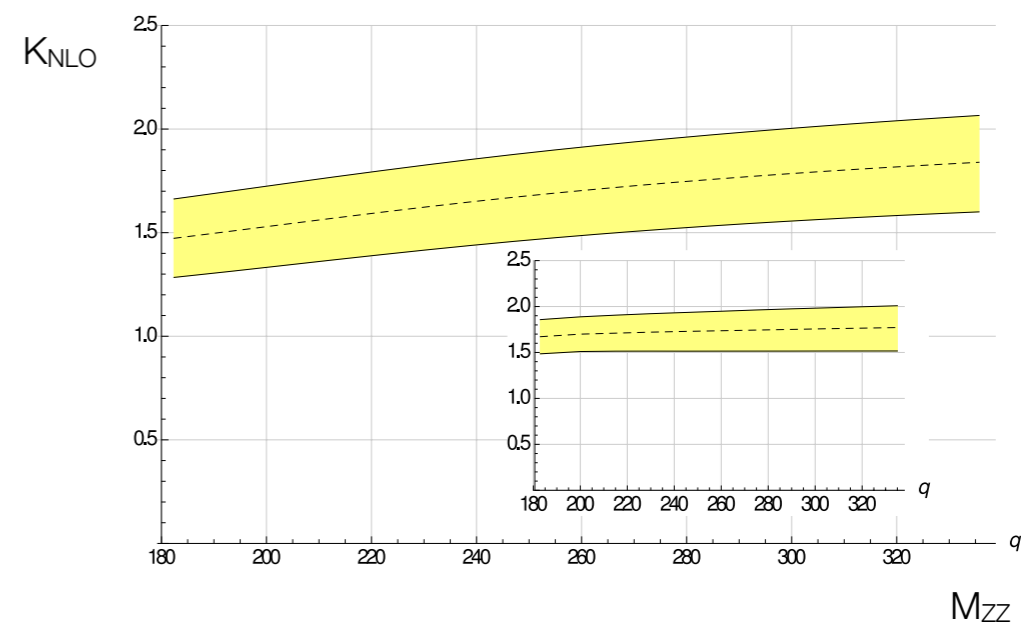
Gluon fusion into a pair of Z-bosons is an irreducible background to Higgs production (the amplitudes interfere). It starts at one-loop, so calculation of even NLO QCD corrections to it is highly non-trivial.

Nevertheless, the NLO QCD corrections to $gg \rightarrow ZZ$ production through massless quark loops were computed; large perturbative corrections (70-90%) were found and the residual uncertainty was estimated to be close to 10 percent.

Top quark loops perhaps are not important for the cross-section but are likely to be relevant for the interference with the Higgs. Recent results for $gg \rightarrow ZZ$ cross-section in the approximation of the infinitely heavy top quark indicate large (1.8) K-factor.



F. Caola, K. Melnikov, R. Rontsch, L. Tancredi



Dowling, Melnikov

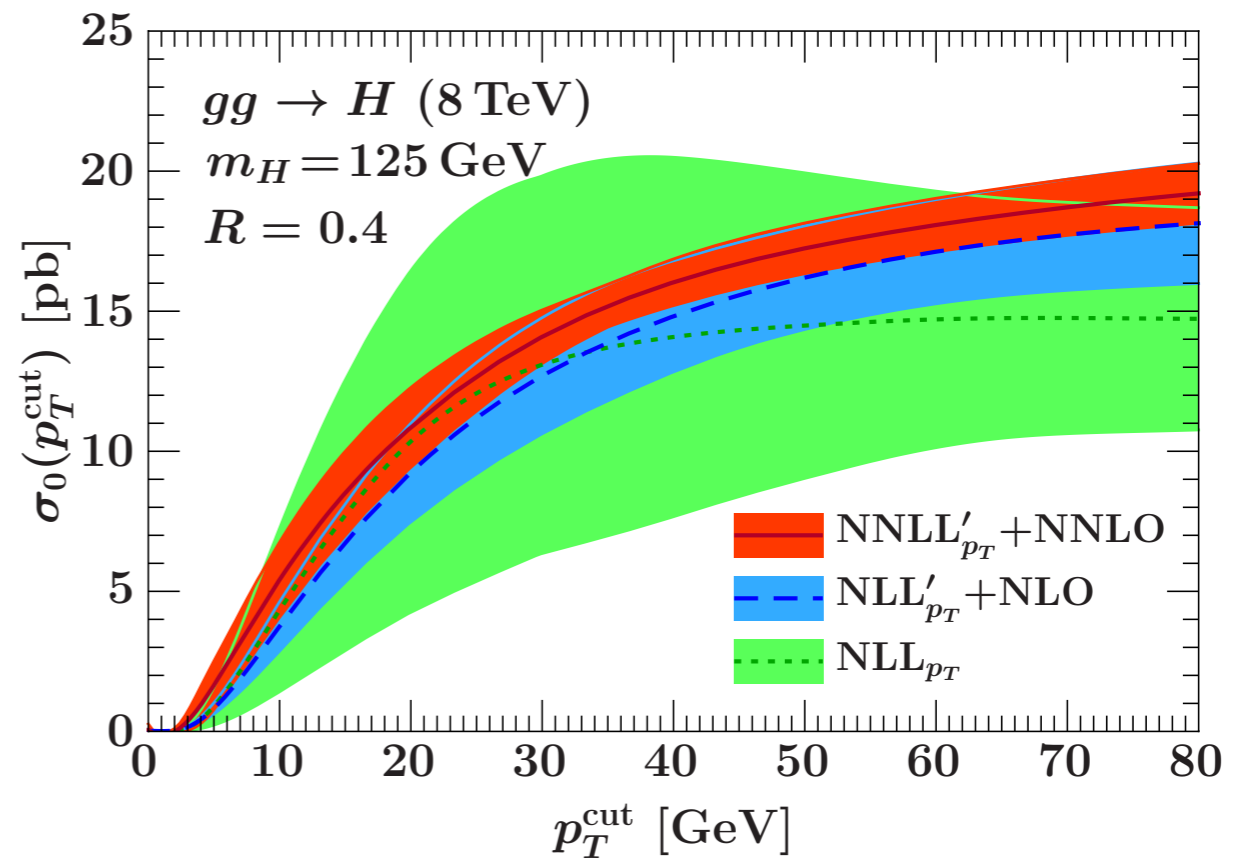
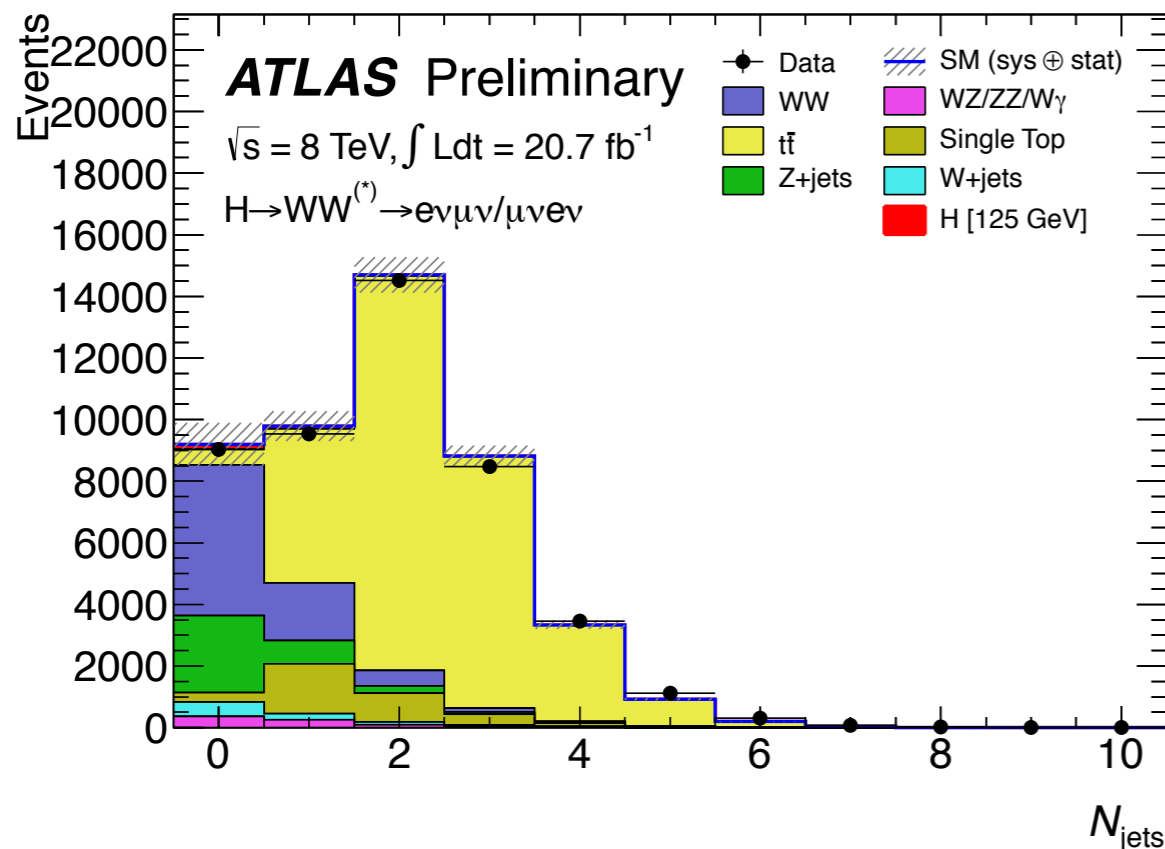
Example: exclusive/fiducial Higgs cross sections

Realistic cross sections

The Higgs boson couplings are extracted from cross sections that are subject to kinematic constraints on the final states. This happens because detectors have only restricted angular coverage and because by selecting final states with particular kinematic properties, certain backgrounds can be significantly reduced.

This, however, requires precision predictions for exclusive/fiducial cross sections, including jet-binning, Higgs boson decays etc, making them highly non-trivial. **Without such predictions, the Higgs couplings can not be extracted from the LHC data with the ultimate precision.**

Jet binning requires jet identification; this may introduce perturbative computations unstable; attempts to resum logarithmically enhanced terms.

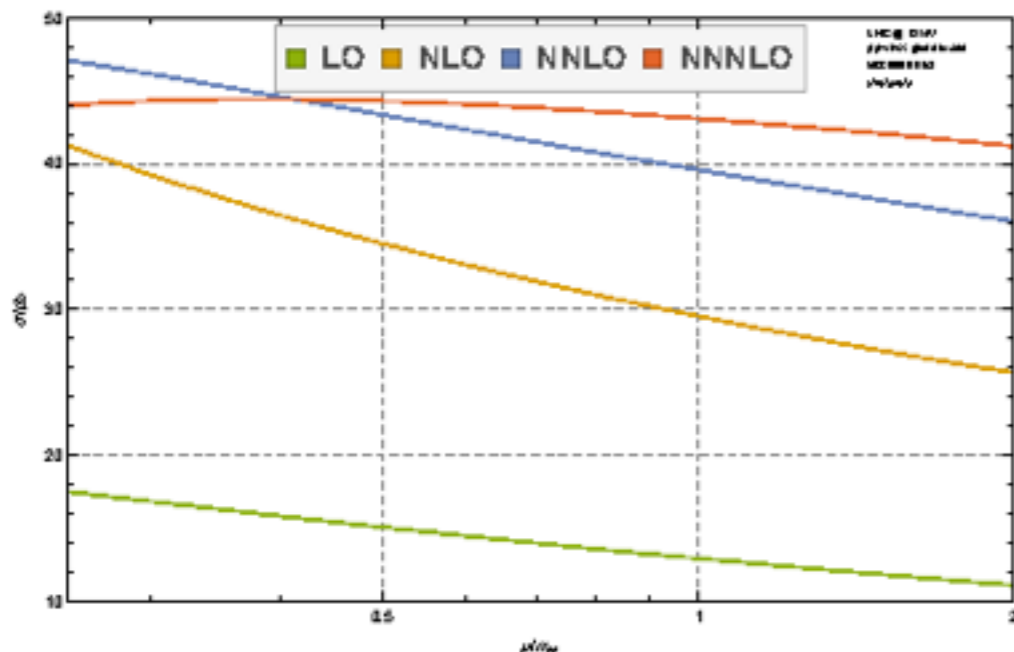
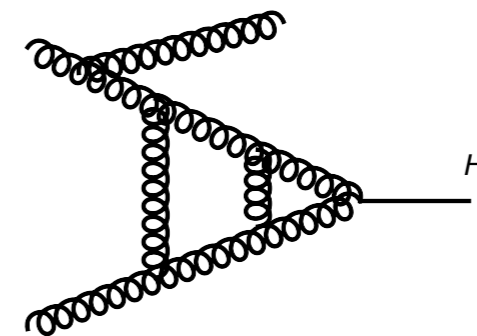
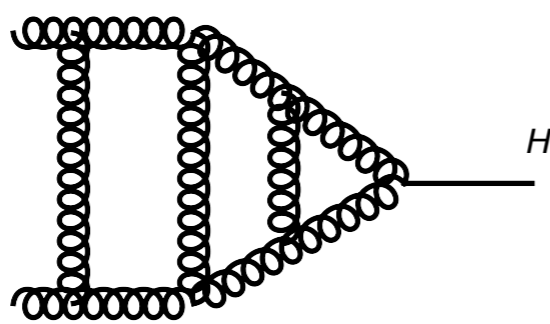


Banfi, Zanderighi, Salam; Tackmann, Zuberi, Walsh; Becher, Neubert

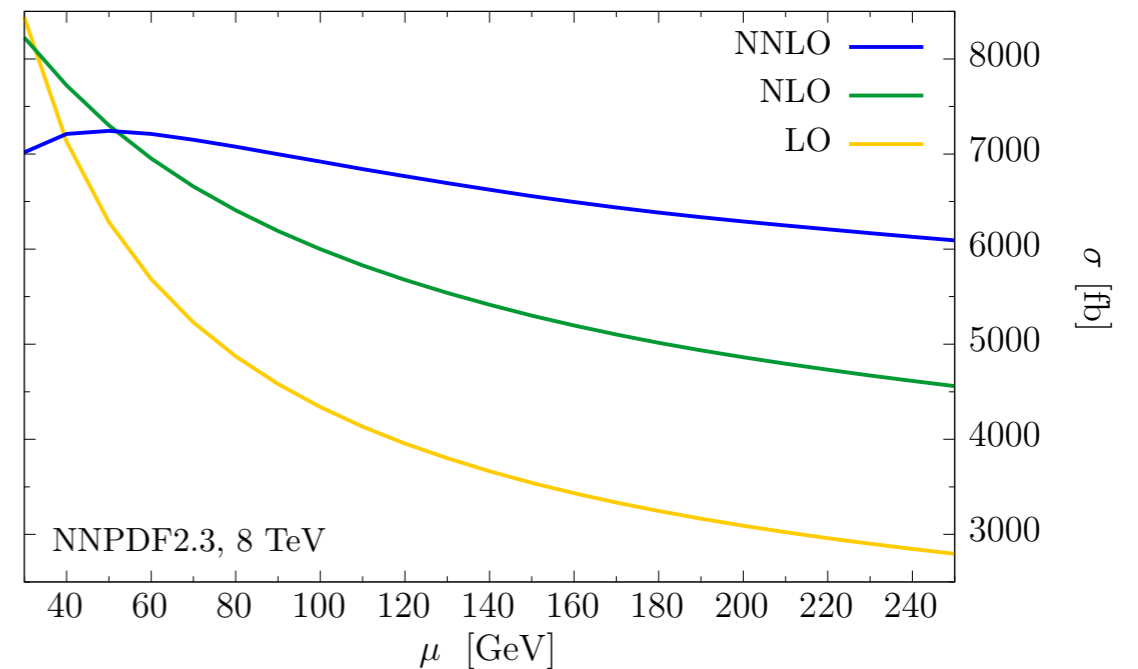
Higgs production: jet-binned cross sections

To obtain the zero-jet cross section for the Higgs production, we subtract the one-jet inclusive cross section from the total inclusive cross section, at matching orders in pQCD.

The inclusive Higgs production was computed recently through N³LO and the H+jet production was computed through NNLO QCD; these are same orders in perturbation theory. **Using these results, one can improve on predictions for jet-binned cross sections.**



Anastasiou, Duhr, Dulat, Furlan, Herzog, Gehrmann, Mistlberger etc.



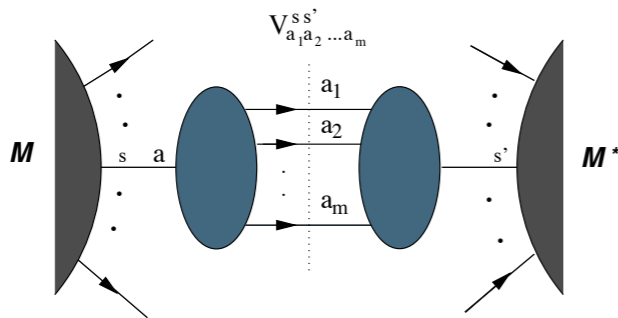
R. Boughezal, F. Caola, K.M., F. Petriello, M. Schulze

NNLO calculations: loops and real emissions

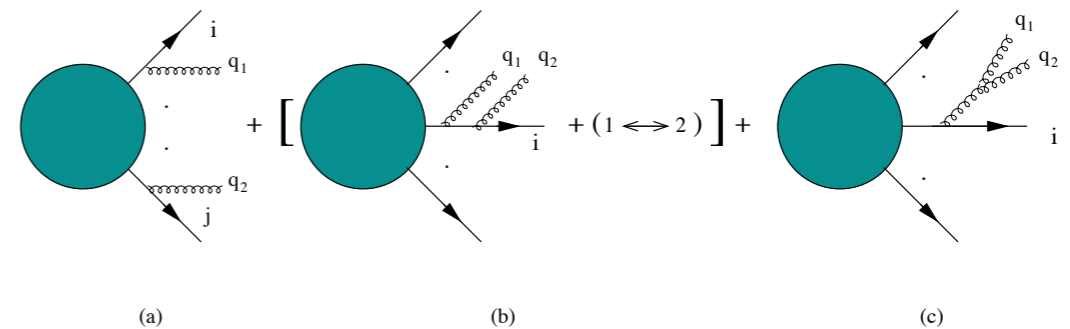
It is easy to recognize that for achieving the cancellation of infra-red and collinear divergences, we only need to integrate over phase-space regions which can generate the singularities.

These are the regions where external particles can become soft and/or collinear to each other and where any measurable differences between final states with different multiplicities become unobservable. In these regions, "singular" matrix elements factorize into universal singular functions and non-singular matrix element of lower multiplicity.

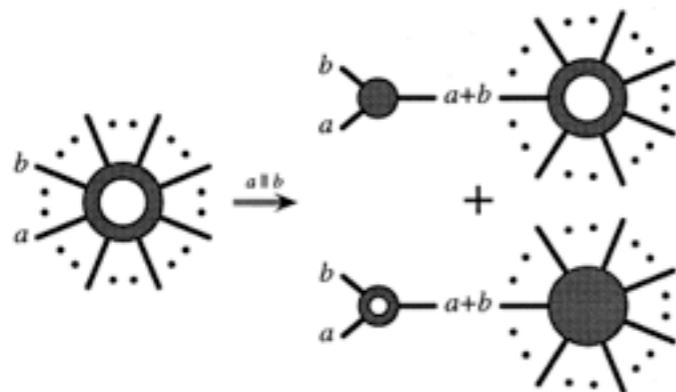
$$\mathcal{M}_{n+i+j} = F_{ij} \mathcal{M}_n$$



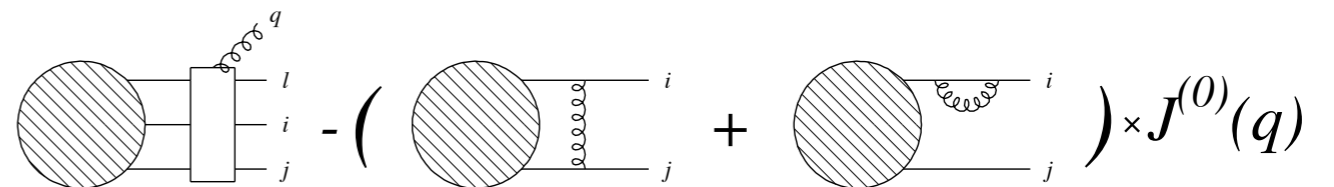
Collinear factorization (Catani, Grazzini)



Soft factorization (Catani, Grazzini)



Collinear factorization at one-loop (Kosower, Uwer)



Soft factorization at one-loop (Catani, Grazzini)

NNLO calculations: loops and real emissions

A universal, simplified form of scattering amplitudes in kinematic regions responsible for the appearance of singularities, together with factorization of multi-particle phase-space, allows us to extract and, eventually, cancel them in a generic, process-independent way.

There are two basic methods familiar from NLO computations: **slicing and subtraction**.

Slicing methods (q_t -subtraction and N-jettiness) are based on splitting the phase-space into regular and singular parts.

$$\int d\Phi_n |\mathcal{M}|^2 F_J = \int_{\text{regular}} d\Phi_n |\mathcal{M}|^2 F_J + \int_{\text{singular}} d\Phi_n |\mathcal{M}|_{\text{approx}}^2 \tilde{F}_J$$

Catani, Grazzini; Bougezhal, Focke, Liu, Petriello; Gaunt, Stahlhofen, Tackmann, Walsh.

Subtraction methods (antenna, improved sector decomposition and projection to Born) are based on subtracting approximate expressions for the amplitude squared from the integrand to make the difference integrable.

$$\int d\Phi_n |\mathcal{M}|^2 F_J = \int d\Phi_n \left(|\mathcal{M}|^2 F_J - |\mathcal{M}|_{\text{approx}}^2 \tilde{F}_J \right) + \int d\Phi_n |\mathcal{M}|_{\text{approx}}^2 \tilde{F}_J$$

Gehrmann-de Ridder, Gehrmann, Glover; Czakon; Bougezhal, Petriello, K.M.
Cacciari, Dreiyer, Kalberg, Salam, Zanderighi

All these methods work and have been used in a large number of recent NNLO QCD computations.

Fiducial cross sections

The results of N³LO computation for inclusive Higgs production, NNLO for the H +j production as well as advances with re-summations of jet-radius logarithms allow one to improve on existing predictions for 0-jet and 1-jet bin cross sections.

For the 13 TeV LHC, using NNPDF2.3, anti-k_T, R=0.5, μ₀=m_H/2, Q_{res} = m_H/2 and accounting for top and bottom mass effects, one finds the following results:

	LHC 13 TeV	$\epsilon^{\text{N}^3\text{LO}+\text{NNLL}+\text{LLR}}$	$\Sigma_{0\text{-jet}}^{\text{N}^3\text{LO}+\text{NNLL}+\text{LLR}}$ [pb]	$\Sigma_{0\text{-jet}}^{\text{N}^3\text{LO}}$	$\Sigma_{0\text{-jet}}^{\text{NNLO}+\text{NNLL}}$
0-jet bin	$p_{t,\text{veto}} = 25 \text{ GeV}$	$0.539^{+0.017}_{-0.008}$	$24.7^{+0.8}_{-1.0}$	$24.3^{+0.5}_{-1.0}$	$24.6^{+2.6}_{-3.8}$
	$p_{t,\text{veto}} = 30 \text{ GeV}$	$0.608^{+0.016}_{-0.007}$	$27.9^{+0.7}_{-1.1}$	$27.5^{+0.5}_{-1.1}$	$27.7^{+2.9}_{-4.0}$
	LHC 13 TeV	$\Sigma_{\geq 1\text{-jet}}^{\text{NNLO}+\text{NNLL}+\text{LLR}}$ [pb]	$\Sigma_{\geq 1\text{-jet}}^{\text{NNLO}}$ [pb]		
$\geq 1\text{-jet}$ bin	$p_{t,\text{min}} = 25 \text{ GeV}$	$21.2^{+0.4}_{-1.1}$	$21.6^{+0.5}_{-1.0}$		
	$p_{t,\text{min}} = 30 \text{ GeV}$	$18.0^{+0.3}_{-1.0}$	$18.4^{+0.4}_{-0.8}$		

- No breakdown of fixed order perturbation theory for $p_T \sim 25\text{-}30 \text{ GeV}$;
- Reliable error estimate from lower orders ; residual errors O(3-5) percent for the two jet bins;
- Re-summed results change fixed-order results within the error bars of the former/latter. There seems to be little difference between re-summed and fixed order results.

A. Banfi, F. Caola, F. Dreyer, P. Monni, G.Salam, G. Zanderighi, F. Dulat

Higgs cross sections: even more fiducial

To go even more fiducial (i.e. realistic), one can let the Higgs decay and compare results with measured cross sections / distributions of the ATLAS collaboration.

Atlas cuts on photons and jets

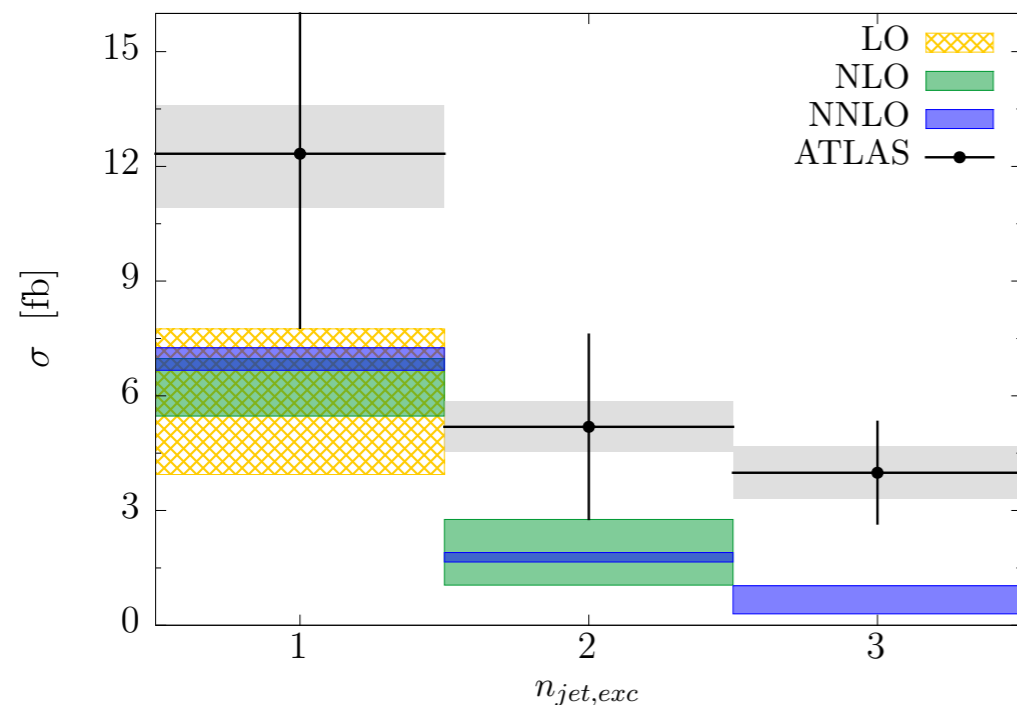
$$\text{anti-}k_t, \quad \Delta R = 0.4, \quad p_{j\perp} = 30 \text{ GeV}, \quad \text{abs}(y_j) < 4.4$$

$$p_{\perp,\gamma_1} > 43.75 \text{ GeV}, \quad p_{\perp,\gamma_2} = 31.25 \text{ GeV}, \quad \Delta R_{\gamma j} > 0.4$$

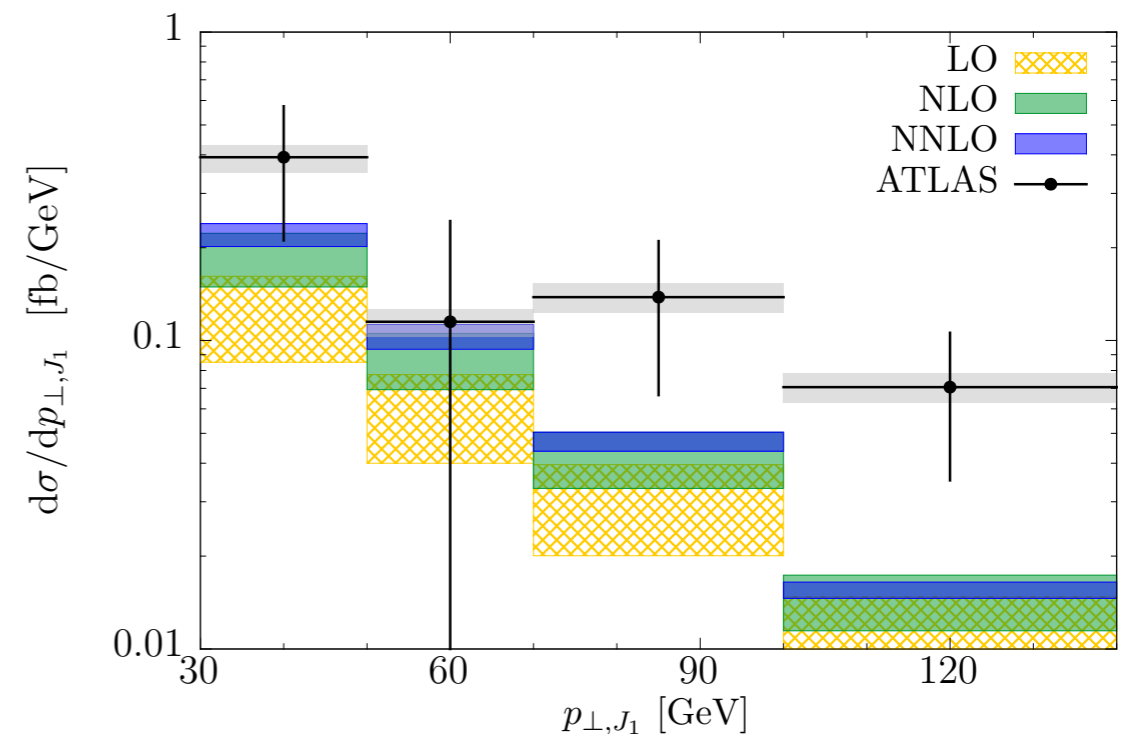
$$\sigma_{1j,\text{ATLAS}}^{\text{fid}} = 21.5 \pm 5.3(\text{stat}) \pm 2.3(\text{syst}) \pm 0.6 \text{ lum fb}$$

$$\sigma_{\text{NNLO}}^{\text{fid}} = 9.46_{-0.84}^{+0.56} \text{ fb}$$

F. Caola, K.M., M. Schulze



Exclusive jet cross sections



Transverse momentum distribution of a leading jet

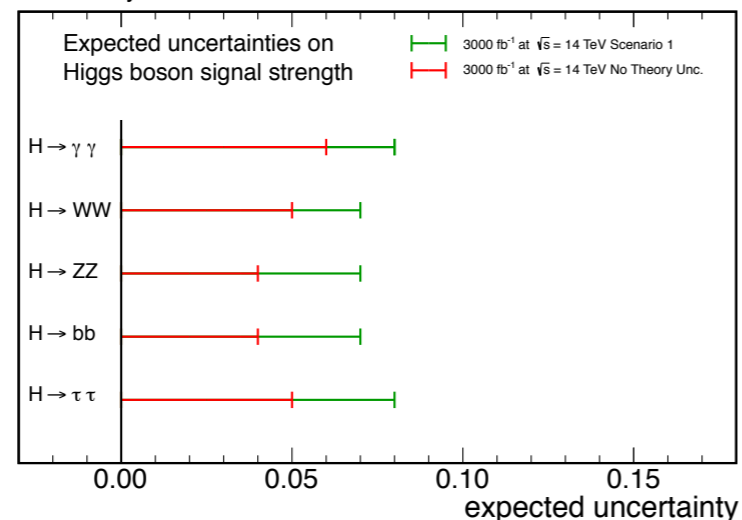
A hadron collider as a machine for precision studies?

Traditionally, hadron colliders played a role of the discovery machines but, given spectacular theoretical advances of recent years, it may be possible to do precision physics at those machines. *A new situation, right in time for the beginning of the Run II.*

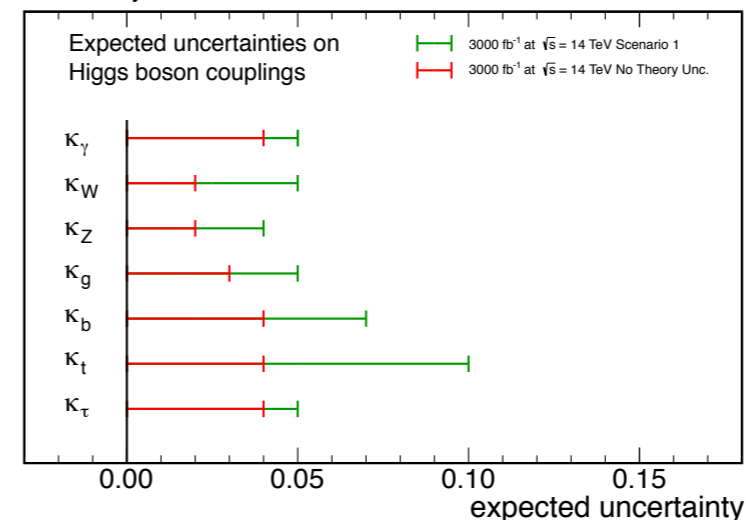
As an illustration, compare theoretical precision on major Higgs production cross sections, that we already have, with experimental precision expected with 3000/fb.

H+0 jet	N ³ LO	O(3-5 %)	10 pb	fully inclusive
H+1 jet	N ² LO	O(7%)	7 pb	fully exclusive; Higgs decays, infinite mass limit
H+2 jet	NLO	O(20%)	1.5 pb	matched/merged
H+3 jet	NLO	O(20%)	0.4 pb	matched/merged/almost
WBF	N ² LO	O(1%)	1.5 pb	exclusive, no VBF cuts
WBF	N ² LO	O(5%)	0.2 pb	exclusive, VBF cuts
ZH, WH	N ² LO	O(2-3%)	O(1) pb	decays to bottom quarks at
ttH	NLO	O(5%)	0.2pb	decays, off-shell effects

CMS Projection

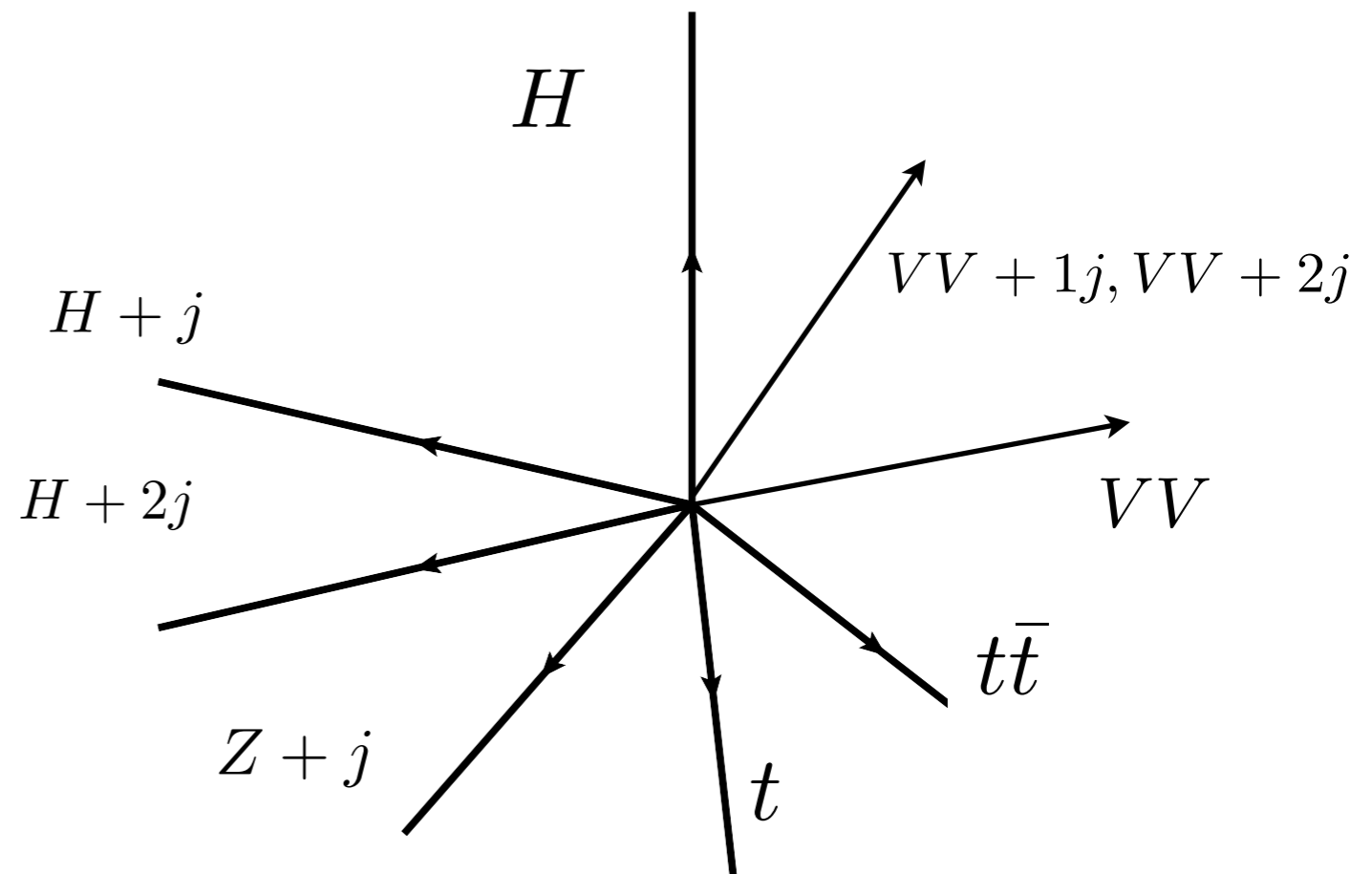
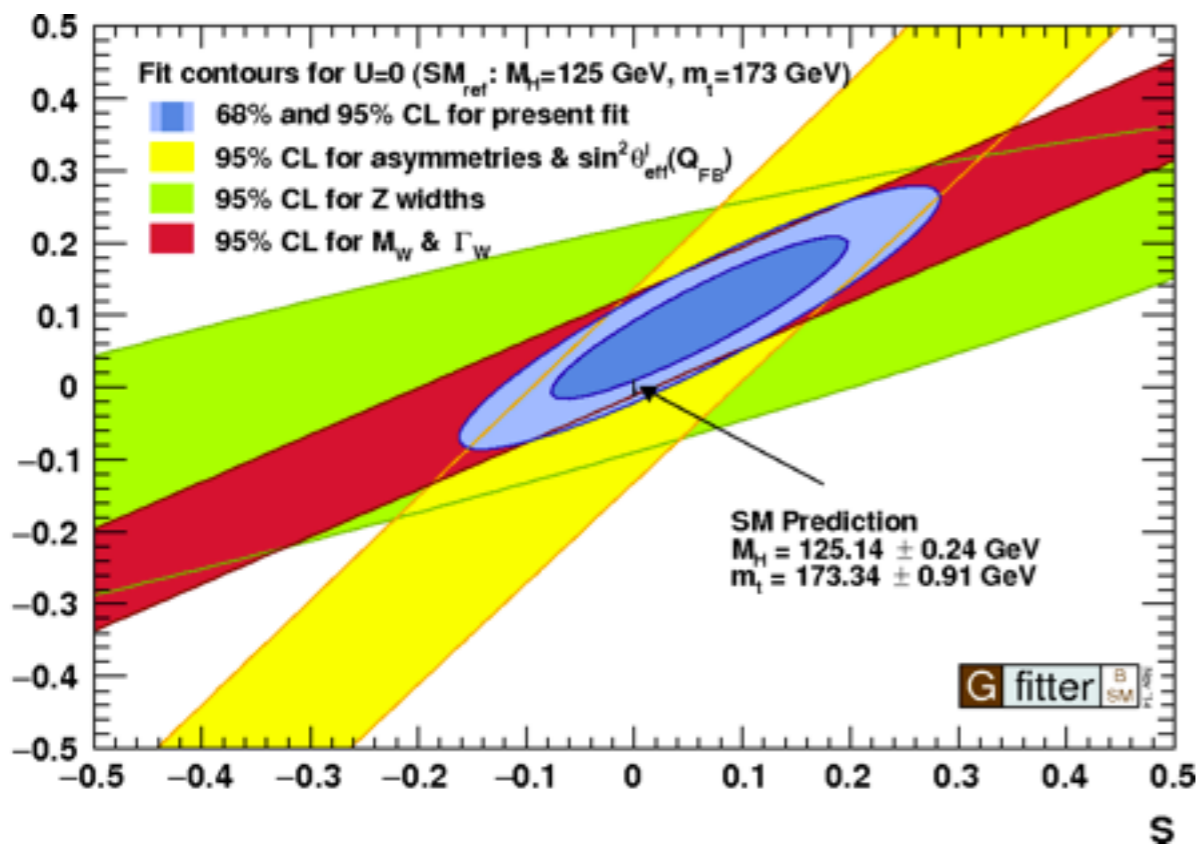


CMS Projection



Future: precision physics at a hadron collider

Precision physics program should aim at facilitating discoveries at the LHC which means that the focus should be on improving precision for **complex processes, across the board**. This will allow us to extract maximal information from the multitude of LHC processes by watching for correlated BSM contributions to many of them. **Interestingly, we are not too far from this goal since we already have high-precision predictions for a large number of complex processes.**



Summary

- 1) Fixed order perturbative computations is the only way to ensure that precision of theory predictions is actually improved. Approximate computations are useful for order-of-magnitude estimates but are insufficient for precision physics.
- 2) Resummations are useful and important. However, we often deal with situations where (resummed) logarithms are neither large nor small. In those cases, several orders in fixed order perturbative QCD take us as far as advanced resummations but with an added bonus of non-logarithmic corrections accounted for.
- 3) Uncertainties in input parameters and parton distribution functions is an important issue; it is difficult to anticipate progress that can be expected.
- 4) Precision can only be achieved for observables for which use of parton showers can be minimized. Minimization of the use of parton showers -- along with their improvements -- should be a priority for precision studies.
- 4) Progress with precision physics can only be achieved through a combined effort of theoretical and experimental communities. Indeed, certain experimental practices (extrapolations, background simulations with parton showers, multi-variate techniques, data-driven background estimates) may introduce biases that are impossible to understand and interpret theoretically at high level of precision.

Conclusion

The LHC is the first hadron collider where outcomes of hard proton collisions can be predicted with a few percent precision for a large number of diverse final states. The possibility to do that is the result of spectacular progress in technology of perturbative QCD that occurred in recent years.

Precision studies at the LHC will allow determination of Higgs couplings with a few percent precision or perhaps even better if theoretical and experimental progress continues at a pace that we have seen in recent years.

Equally important, progress with precision predictions for complex multi-particle final states should allow for broad-band searches for (correlated) deviations in multitude of kinematic distributions that can be measured for various final states at the LHC. Such correlated deviations -- if discovered -- will signal the presence of physics beyond the SM which is too heavy to be observed at the LHC and, in this way, will allow us to determine the energy scale where the Standard Model breaks down.

Further improvements of theoretical methods are required to pursue this research program. They include understanding massive loops, development of two-loop unitarity and improvements in the efficiency of subtraction methods.

Moreover, to fully benefit from these theoretical developments, we will need to better understand parameters that enter calculation of cross sections (PDFs, masses, couplings, etc.), to include electroweak corrections, to work only with realistic final states and fiducial cross sections and to understand the limitations of various approximations that we currently use in theoretical computations.